The Plant Cell, Vol. 16, 1979–2000, August 2004, www.plantcell.org © 2004 American Society of Plant Biologists

A Systemic Small RNA Signaling System in Plants

Byung-Chun Yoo,[a,1] Friedrich Kragler,[a,1] Erika Varkonyi-Gasic,[b] Valerie Haywood,[a] Sarah Archer-Evans,[a] Young Moo Lee,[c] Tony J. Lough,[b] and William J. Lucas[a,2]

[a] Section of Plant Biology, Division of Biological Sciences, University of California, Davis, California 95616
[b] AgriGenesis Biosciences, Auckland, New Zealand
[c] Molecular Structure Facility, University of California, Davis, California 95616

Systemic translocation of RNA exerts non-cell-autonomous control over plant development and defense. Long-distance delivery of mRNA has been proven, but transport of small interfering RNA and microRNA remains to be demonstrated. Analyses performed on phloem sap collected from a range of plants identified populations of small RNA species. The dynamic nature of this population was reflected in its response to growth conditions and viral infection. The authenticity of these phloem small RNA molecules was confirmed by bioinformatic analysis; potential targets for a set of phloem small RNA species were identified. Heterografting studies, using spontaneously silencing coat protein (*CP*) plant lines, also established that transgene-derived siRNA move in the long-distance phloem and initiate *CP* gene silencing in the scion. Biochemical analysis of pumpkin (*Cucurbita maxima*) phloem sap led to the characterization of *C. maxima* Phloem SMALL RNA BINDING PROTEIN1 (CmPSRP1), a unique component of the protein machinery probably involved in small RNA trafficking. Equivalently sized small RNA binding proteins were detected in phloem sap from cucumber (*Cucumis sativus*) and lupin (*Lupinus albus*). PSRP1 binds selectively to 25-nucleotide single-stranded RNA species. Microinjection studies provided direct evidence that PSRP1 could mediate the cell-to-cell trafficking of 25-nucleotide single-stranded, but not double-stranded, RNA molecules. The potential role played by PSRP1 in long-distance transmission of silencing signals is discussed with respect to the pathways and mechanisms used by plants to exert systemic control over developmental and physiological processes.

INTRODUCTION

In eukaryotic organisms, a paradigm is emerging in which RNA functions as non-cell-autonomous signaling molecules (Fire et al., 1998; Jorgensen et al., 1998; Lucas et al., 2001; Hannon, 2002; Winston et al., 2002; Wu et al., 2002; Zamore, 2002; Roignant et al., 2003). In plants, a role for non-cell-autonomous RNA has been established in terms of systemic signaling associated both with RNA interference (RNAi) (Palauqui et al., 1997; Jorgensen et al., 1998; Voinnet et al., 1998; Fagard and Vaucheret, 2000; Vance and Vaucheret, 2001; Mlotshwa et al., 2002) and development (Ruiz-Medrano et al., 1999; Xoconostle-Cázares et al., 1999; Kim et al., 2001).

Plasmodesmata (PD), the intercellular organelles of the plant kingdom (Lucas, 1995; Jackson, 2000; Zambryski and Crawford, 2000; Haywood et al., 2002), serve as the conduit through which proteins and RNA-protein complexes move, cell to cell, to exert supracellular control (Lucas et al., 1995; Sessions et al., 2000; Nakajima et al., 2001; Kim et al., 2002, 2003; Wada et al., 2002; Schiefelbein, 2003). The vascular system, and specifically the specialized cell types of the phloem, provide the pathway for the long-distance translocation of non-cell-autonomous proteins and RNA-protein complexes to distantly located tissues and organs (Fisher et al., 1992; Palauqui et al., 1997; Golecki et al., 1998, 1999; Jorgensen et al., 1998; Ruiz-Medrano et al., 1999; Xoconostle-Cázares et al., 1999; Kim et al., 2001). Delivery of such informational macromolecules into and out of the phloem translocation stream appears to occur through PD (Balachandran et al., 1997; Aoki et al., 2002; van Bel, 2003).

The protein machinery involved in RNAi is currently under intense investigation (Dalmay et al., 2000, 2001; Mourrain et al., 2000; Sijen et al., 2001; Wassenegger, 2002; Tang et al., 2003). It is now evident that an RNase III–type enzyme, termed Dicer in animals (Hammond et al., 2000; Bernstein et al., 2001) and Dicer-like (DCL) in plants (Schauer et al., 2002; Papp et al., 2003; Tang et al., 2003), is pivotal to this process. Dicer enzymes bind and cleave double-stranded RNA (dsRNA) into 21- to 25-nucleotide dsRNA species (Hamilton and Baulcombe, 1999; Zamore et al., 2000; Elbashir et al., 2001). These small RNA cleavage products then function as sequence-specific small interfering RNA (siRNA) or microRNA (miRNA) involved in transcript turnover, cleavage, or translational control (Olsen and Ambros, 1999; Hutvagner et al., 2001; Hutvagner and Zamore, 2002; Llave et al., 2002a, 2002b; Reinhart et al., 2002; Aukerman and Sakai, 2003; Khvorova et al., 2003; Kidner and Martienssen, 2003; Lim et al., 2003). In plants, the cell-to-cell and systemic spread of RNAi is considered to occur through PD (Voinnet et al., 1998; Lucas et al., 2001; Mlotshwa et al., 2002; Himber et al., 2003) and the phloem (Palauqui et al., 1997; Jorgensen et al., 1998; Fagard and

[1] These authors contributed equally to this work.
[2] To whom correspondence should be addressed. E-mail wjlucas@ucdavis.edu; fax 530-752-5410.
The author responsible for distribution of materials integral to the findings presented in this article in accordance with the policy described in the Instructions for Authors (www.plantcell.org) is: William J. Lucas (wjlucas@ucdavis.edu).
Article, publication date, and citation information can be found at www.plantcell.org/cgi/doi/10.1105/tpc.104.023614.

Vaucheret, 2000; Vance and Vaucheret, 2001; Klahre et al., 2002; Mallory et al., 2003), respectively; however, the RNA species and underlying mechanism of trafficking remain to be elucidated (Vance and Vaucheret, 2001; Hamilton et al., 2002; Klahre et al., 2002; Mlotshwa et al., 2002; Himber et al., 2003; Mallory et al., 2003).

In this study, we performed a detailed analysis of phloem sap collected from various plants and identified populations of small RNA species likely involved in systemic signaling processes. The dynamic nature of this population was reflected in its response to viral infection and growth conditions. Experiments conducted with spontaneously silencing plant lines and viral-infected tissues confirmed the presence of transgene- and viral-derived siRNA in the phloem. Bioinformatic analyses performed on a phloem small RNA–derived database identified potential targets for many of these phloem small RNA species. Biochemical analysis of pumpkin (*Cucurbita maxima*) phloem sap led to the characterization of *C. maxima* Phloem SMALL RNA BINDING PROTEIN1 (CmPSRP1), a unique component of the protein machinery that binds selectively to small single-stranded RNA (ssRNA) species. Evidence is presented that PSRP1 mediates cell-to-cell trafficking of small ssRNA but not dsRNA molecules. These results are discussed in terms of the long-distance transmission of silencing signals in plants.

RESULTS

Cucurbit Phloem Sap Contains a Population of Small RNA Molecules

Earlier efforts to identify the nature of the RNA species that serves as the systemic-signaling agent(s) were based on analyses conducted on whole leaf tissues (Voinnet et al., 1998; Mallory et al., 2001; Guo and Ding, 2002; Hamilton et al., 2002; Klahre et al., 2002; Mlotshwa et al., 2002), rather than directly on the phloem translocation stream. In this study, we used cucurbits from which analytical quantities of phloem sap could be collected (Balachandran et al., 1997; Golecki et al., 1998; Yoo et al., 2002); an added advantage of this system was that protocols

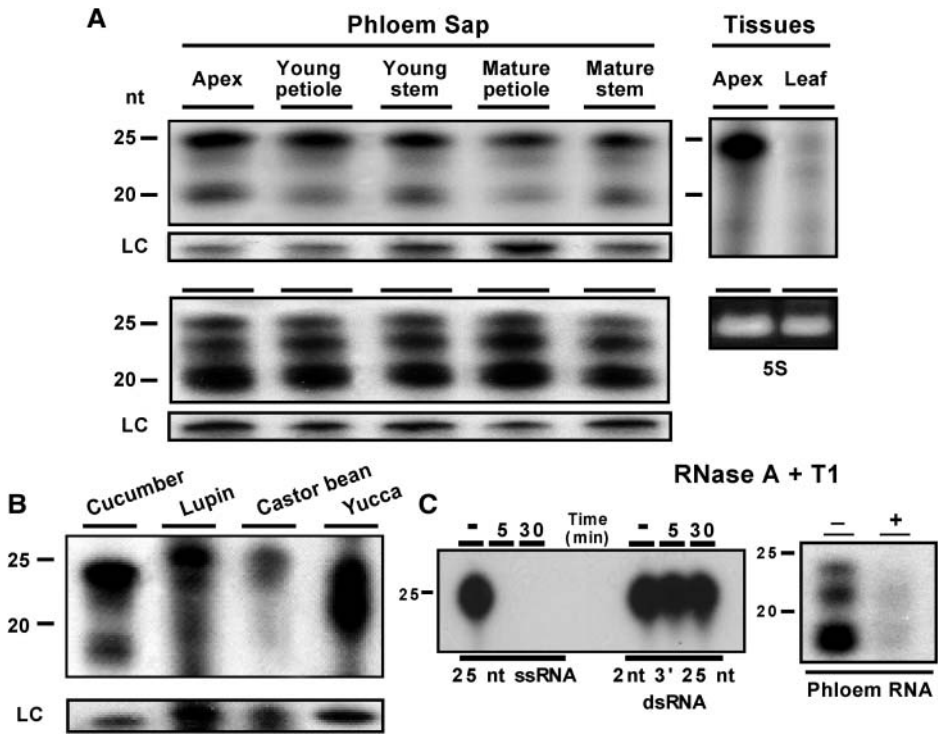

Figure 1. Small RNA Population Detected in the Pumpkin Phloem Translocation Stream.

(A) Small RNA species present within the phloem sap and vegetative tissues of pumpkin were extracted, end-labeled with ^{32}P-phosphate, separated using PAGE, and then visualized by autoradiography. Left top and bottom panels: samples from summer- and winter-grown plants, respectively. Loading control (LC): a constant high molecular weight band present in the unfractionated phloem sap RNA was used for between sample calibration. Right top and bottom panels: apical and mature leaf tissues from summer-grown plants and ethidium bromide–stained 5S rRNA as loading control, respectively (0.3 μg per lane). nt, nucleotides.

(B) Small RNA species detected in the phloem sap of cucumber, white lupin, caster bean, and yucca.

(C) ssRNA-specific RNase assay performed on control (synthetic 25-nucleotide ssRNA and 2-nucleotide 3′ 25-nucleotide dsRNA) and phloem small RNA preparations. Note the absence of signal associated with the synthetic 25-nucleotide ssRNA and low residual level in the phloem RNA population after treatment.

exist for the isolation and analysis of phloem-mobile proteins and RNA (Ruiz-Medrano et al., 1999; Xoconostle-Cázares et al., 1999; Yoo et al., 2002). Our analysis of pumpkin phloem sap demonstrated the presence of an endogenous population of small RNA, and as illustrated in Figure 1A, these small RNA species ranged from ~18 to 25 nucleotides in size.

The pattern of small RNA was found to be constant for plants grown under similar conditions; however, differences were detected between summer- and winter-grown plants. A comparison of the small RNA species present in leaves, the vegetative apex, and phloem sap (collected from various tissues) indicated that each displayed a characteristic pattern in terms of the relative abundance of the small RNA molecules (Figure 1A). Phloem sap was collected from an additional four plant species and analyzed for the presence of small RNA molecules; cucumber (*Cucumis sativus*), lupin (*Lupinus albus*), castor bean (*Ricinus communis*), and yucca (*Yucca filamentosa*) phloem all contained small RNA profiles that differed among these species (Figure 1B). Enzymatic assays indicated that these phloem small RNA species appeared to exist predominantly as ssRNA (Figure 1C).

Phloem Sap Contains Authentic siRNA and miRNA Species

Biochemical assays were next performed on purified phloem small RNA samples to test for the involvement of an RNase III–type enzyme. The presence of 5′-phosphate was demonstrated by shrimp alkaline phosphatase treatment; the observed reduction in RNA electrophoretic mobility for both synthetic 24-nucleotide RNA (control: 5′-phosphate and 3′-hydroxyl group) and gel-purified phloem sap small RNA was consistent with removal of the negatively charged 5′-phosphate group (data not shown). Treatment of an aliquot of these same small RNA preparations with RNA ligase resulted in circularization and concatenation. These results indicate that the small RNA species extracted from the cucurbit phloem sap most probably contain 5′-phosphate and 3′-hydroxyl terminal residues (i.e., chemical

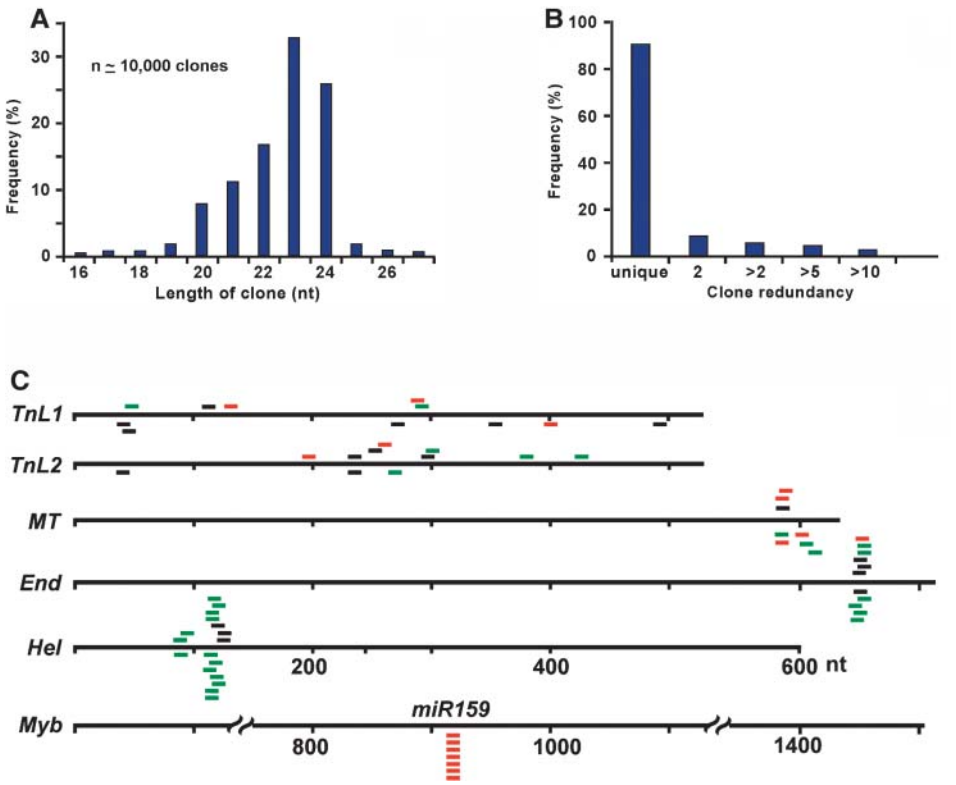

Figure 2. Molecular Size, Complexity, and Potential Targets for Phloem Small RNA Species.

(A) and **(B)** Size distribution and complexity, respectively, of the small RNA species contained within a phloem database (10,000 clones) generated from summer-grown pumpkin (sap collected from mature petioles). nt, nucleotides.

(C) Representative putative target genes of phloem small RNA with identified homology to cucurbit ESTs and/or Arabidopsis genes. Distribution of sense (above target gene; black, 0; green, 1; red, 2; and blue, 3 mismatches, respectively) and antisense (below target gene; colors as described for sense) clones directed against the indicated genes. Targets: cucurbit *TnL1* and *TnL2*; cucurbit small RNA identical to Arabidopsis miR159 proposed to target a *MYB* transcription factor (GenBank accession number At2g32460); putative *MT* (homologous to a spinach gene [GenBank accession number AF237633]); bifunctional *End* (homologous to a *Zinnia elegans* gene [GenBank accession number O80326]) and RNA *Hel* (homologous to a *Vigna radiata* gene [GenBank accession number AF156667]). The size classes directed against the *TnL* and *Myb* genes were centered on 21 nucleotides, whereas those associated with *MT*, *End*, and *Hel* were in the 23- to 24-nucleotide range.

Table 1. Identification of Putative Arabidopsis miRNA Orthologs of Cloned Cucurbit Phloem miRNA Molecules

miRNA[a]	Sequence (5′/3′)	Databases with FASTA Hits	Mismatches[b]	Direction[c]	Arabidopsis Best Hit	Description[d]	Target Gene Family
miR156[e]	TGACAGAAGAG AGTGAGCAC	Actinidia Arabidopsis Populus	1	R	At1g69170	Squamosa-promoter binding protein–related, similar to squamosa-promoter binding protein 1 GI:1183865 from (*Antirrhinum majus*)	SQUAMOSA-PROMOTER BINDING PROTEIN (SBP-like proteins)
		Actinidia Arabidopsis Eucalyptus Glycine Gossypium Malus Zea	1	R	At2g42200	Squamosa-promoter binding protein–related	SBP-like proteins
		Arabidopsis Eucalyptus Populus	1	R	At5g50670	Expressed protein, contains similarity to squamosa promoter binding protein	SBP-like proteins
		Arabidopsis Eucalyptus Pinus Triticum Vitis	1 to 2	R	At5g43270	Squamosa promoter binding protein–related 2 (emb/CAB56576.1)	SBP-like proteins
		Glycine Lolium Medicago Pinus Zea	1 to 3	R	At1g53160	Transcription factor–related, similar to GB:X92369 from (*A. majus*)	SBP-like proteins
		Actinidia Eucalyptus Lycopersicon Populus Vaccinium	2 to 3	R	At3g15270	Squamosa promoter binding protein–related 5, identical to GB:CAB56571 from (Arabidopsis)	SBP-like proteins
miR159[e]	TTTGGATTGAA GGGAGCTCTA	Arabidopsis Festuca Populus Triticum	2 to 3	R	At5g06100	Myb family transcription factor, contains Pfam profile: PF00249 myb DNA binding domain	MYB transcription factors
		Arabidopsis Populus Vitis	3	R	At3g11440	Myb family transcription factor, contains Pfam profile: PF00249 myb-like DNA binding domain	MYB transcription factors
Similar to miR167[e]	TCAAGCTGC CAGCATGAT CTGA	Actinidia Arabidopsis Eucalyptus Glycine Lolium Malus Medicago Pinus Populus Triticum Vaccinium Zea	3	R	At1g30330	ARF6 (ARF6) mRNA	Auxin response factors
		Arabidopsis Glycine Medicago	3	R	At5g37020	Auxin response factor 8 (ARF8) mRNA	Auxin response factors

(Continued)

Table 1. (continued).

miRNA[a]	Sequence (5′/3′)	Databases with FASTA Hits	Mismatches[b]	Direction[c]	Arabidopsis Best Hit	Description[d]	Target Gene Family
miR171[f]	TGATTGAGCCG CGCCAATATC	Actinidia Arabidopsis Glycine Lotus Medicago Pinus Populus Zea	0	R	At4g00150	Scarecrow-like transcription factor 6 (SCL6)	GRAS domain transcription factors (SCARECROW-like)
		Cucurbita Eucalyptus Glycine Lotus Lycopersicon Populus	0 to 3	R	At4g36710	Scarecrow transcription factor family	GRAS domain transcription factors (SCARECROW-like)

[a] Cloned and sequenced phloem sap small RNAs were interrogated by conducting FASTA analyses with the sense and complementary sequence directed against an EST-derived database. Sequences within each of these data sets were then mapped by TBLASTX against Arabidopsis genes. miR171 cloned from Arabidopsis apices was used as a control to validate our miRNA target identification process.

[b] Bulges and G:U wobbles were included as mismatches in these analyses.

[c] Direction: R represents the reverse, or complementary, reading frame.

[d] Descriptions are from The Arabidopsis Information Resource ([TAIR]; http://www.arabidopsis.org/info/ontologies).

[e] Phloem-mobile miRNA species.

[f] Not detected in phloem sap.

properties consistent with their being generated by RNase III activity) (Tang et al., 2003).

To further confirm the authenticity of these phloem small RNA molecules, sap was next collected from petioles of mature summer-grown plants and the small RNA population extracted and cloned to generate a bioinformatic database. The resultant distribution of the various size classes, presented in Figure 2A, was consistent with the observed phloem small RNA pattern (Figure 1A). Interrogation of these clones revealed an underlying complexity associated with this population (Figure 2B). Using available plant genome databases, it was possible to identify potential targets for several of these phloem mobile small RNA molecules (Figure 2C). The distribution of the small RNA along the transposon-like 1 (*TnL1*) and *TnL2* target sequences suggested the action of siRNA. The small RNA patterns observed for cucurbit ESTs of a putative methyltransferase ([*MT*]; homologous to a spinach gene), bifunctional endonuclease ([*End*]; homologous with a *Zinnia elegans* gene), and RNA helicase ([*Hel*]; homologous with a *Vigna radiata* gene) could reflect a novel method for small RNA targeting.

Interrogation of these plant databases, against characterized plant miRNA (Reinhart et al., 2002), also identified several putative *Arabidopsis thaliana* orthologs contained within the phloem small RNA library; representative examples are presented in Figure 2C and Table 1. As shown in Figure 3, RNA gel blot analysis established that miR156, miR159, and miR167 were detected in RNA extracted from both plant tissues and phloem sap, whereas miR171 was absent from the phloem miRNA population. No hybridization was detected with end-labeled sense oligonucleotides. Taken together, these results implicate the involvement of both siRNA and miRNA in phloem-mediated long-distance regulation of gene function in plants.

Viral *Coat Protein*–Specific siRNA Carried in Phloem of Spontaneously Silencing Plants

Our current understanding of RNA silencing in plants is based primarily on experiments performed using leaf tissues expressing transgenes (Palauqui et al., 1997; Voinnet et al., 1998; Mlotshwa et al., 2002). Such a transgenic system was next used to test for the presence, in the phloem, of the associated siRNA. Spontaneously silencing and nonsilencing transgenic yellow crookneck squash (*Cucurbita pepo*) lines, expressing a viral coat protein (*CP*) gene (Pang et al., 2000), were examined by RNA gel blot analysis. As illustrated in Figure 4, we could detect *CP* siRNA, in the 23-nucleotide size range, in mature leaves and within the phloem of silenced lines; however, no such siRNA was detected from either nonsilenced *CP* transgenic or wild-type tissue. Note that as comparable small RNA profiles were observed in the phloem of wild-type and *CP* silenced squash plants (Figure 4C), it would appear that the *CP* siRNA is not a dominant species in the phloem translocation stream of such spontaneously silencing plants. Finally, both sense and antisense *CP* siRNA were detected in the phloem sap at similar levels (Figure 4B), suggesting that the dsRNA form may predominate. However, RNase enzyme assays revealed the absence of this dsRNA form (Figure 4D).

Grafting experiments were next performed to further test whether these *CP* siRNA were bone fide constituents of the

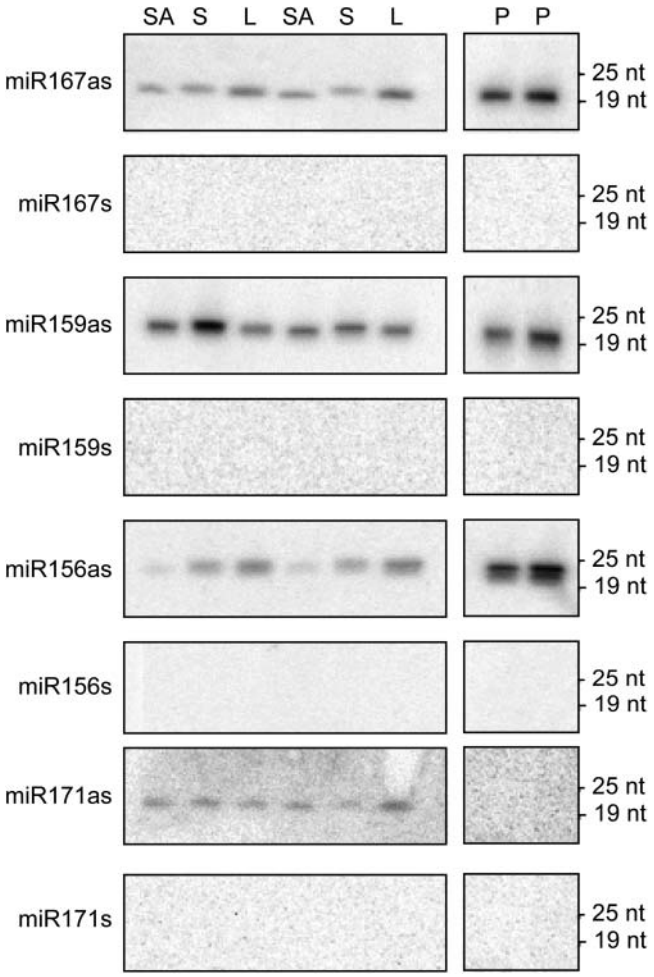

Figure 3. RNA Gel Blot Analysis of miRNA in Various Pumpkin Tissues and Phloem Sap.

Total RNA was extracted from shoot apices (SA), stem tissue (S), mature leaves (L), and phloem sap (P) and the small RNA species extracted by size fractionation. Duplicate RNA samples were separated on a denaturing polyacrylamide gel, transferred to Hybond-N^+ nylon membrane, and hybridized with either radiolabeled DNA sense (s) or antisense (as) probes complementary to four identified plant miRNAs (miR156, miR159, miR167, and miR171; Reinhart et al., 2002). Position of RNA oligonucleotide standards is indicated on the right. RNA loading was normalized by spectrometry, and 2 μg of small RNA was used per lane. nt, nucleotides.

phloem translocation stream, as opposed to wound-induced contaminants (Knoblauch and van Bel, 1998; van Bel, 2003) derived from neighboring silenced tissues. Phloem sap collected from cucumber scions grafted onto either wild-type or nonsilencing *CP* transgenic squash lines was free of *CP* siRNA (Figure 4E). By contrast, equivalent experiments performed with cucumber (scion) and the spontaneously silencing squash line 127 (stock) revealed the presence of both sense and antisense *CP* siRNA in the phloem sap taken from both stock and scion tissues.

Parallel experiments were conducted in which line 22(NS) was grafted onto spontaneously silencing stocks; homografts were used as controls. Three weeks after grafting, entire scion apices (terminal 1 cm of sink tissue) were excised and analyzed for *CP* transcripts and siRNAs. Apical tissues from 3(S) plants exhibited low *CP* mRNA and high siRNA signal; the converse was observed with 22(NS) scions (Figure 4F). The level of *CP* mRNA in the apex of heterografted 3(S):22(NS) squash plants was reduced to levels equivalent to those detected in 3(S) tissues. Consistent with 3(S) stock-induced systemic silencing, a weak *CP* siRNA signal was detected by RNA gel blot analysis (Figure 4F).

RNA gel blot and RT-PCR analyses were next conducted to ascertain whether the phloem sap collected from these transgenic melon lines also contained other forms of *CP* RNA. No full-length *CP*-specific signal was detected in our RNA gel blot hybridization analysis (data not shown), suggesting that, if present, any such RNA would be there at very low levels. This conclusion was supported by RT-PCR performed using a range of *CP*-specific primer sets (designed to amplify both full-length and internal *CP* fragments). No signal was amplified from RNA samples extracted from wild-type plants, but sense and antisense transcripts were detected in both mature leaves and phloem sap of spontaneously silencing squash plants (Figure 4G, lines 3[S] and 127[S]). Although the signal associated with the antisense *CP* transcript was always weak, it could be routinely detected. Equivalent analysis performed on squash line 22(NS) identified similar signals.

Phloem of Viral-Infected Plants Contains a High Level of siRNA

Plants use RNA silencing as a surveillance mechanism to protect against viral attack (Jorgensen et al., 1998; Voinnet, 2001; Mlotshwa et al., 2002). Viral infection of cucurbits was next used to test for the presence of viral-directed siRNA in the phloem during such a challenge. Data from our molecular analysis of the phloem sap, collected from *Cucumber yellows closterovirus* (CuYV)-infected pumpkin (Hartono et al., 2003), are presented in Figure 5. These results show that sap from infected plants contained both sense and antisense siRNA (20- to 21-nucleotide size class) directed along the length of the viral genome (Figure 5A). The phloem sap also contained CuYV transcripts (data not shown), probably reflecting a dynamic balance between RNAi-based surveillance and viral infection. In contrast with the spontaneously silencing *CP* lines, a comparison of the small RNA present in the phloem of healthy and infected plants indicated a significant shift in this population, resulting from an increase in siRNA derived from the viral RNA (Figure 5B). These findings are also consistent with the hypothesis that small RNA species participate in the systemic response of the plant to viral challenge.

PSRP1 Is a Phloem Small RNA Binding Protein

The phloem sap was earlier shown to contain proteins involved in mRNA trafficking (Xoconostle-Cázares et al., 1999). We next investigated whether the phloem translocation stream contains proteins that bind specifically to small RNA. RNA overlay assays were first performed using previously identified phloem-mobile mRNAs (Ruiz-Medrano et al., 1999) to identify the spectrum of phloem proteins from pumpkin, cucumber, and lupin that could bind to these transcripts. An example based on

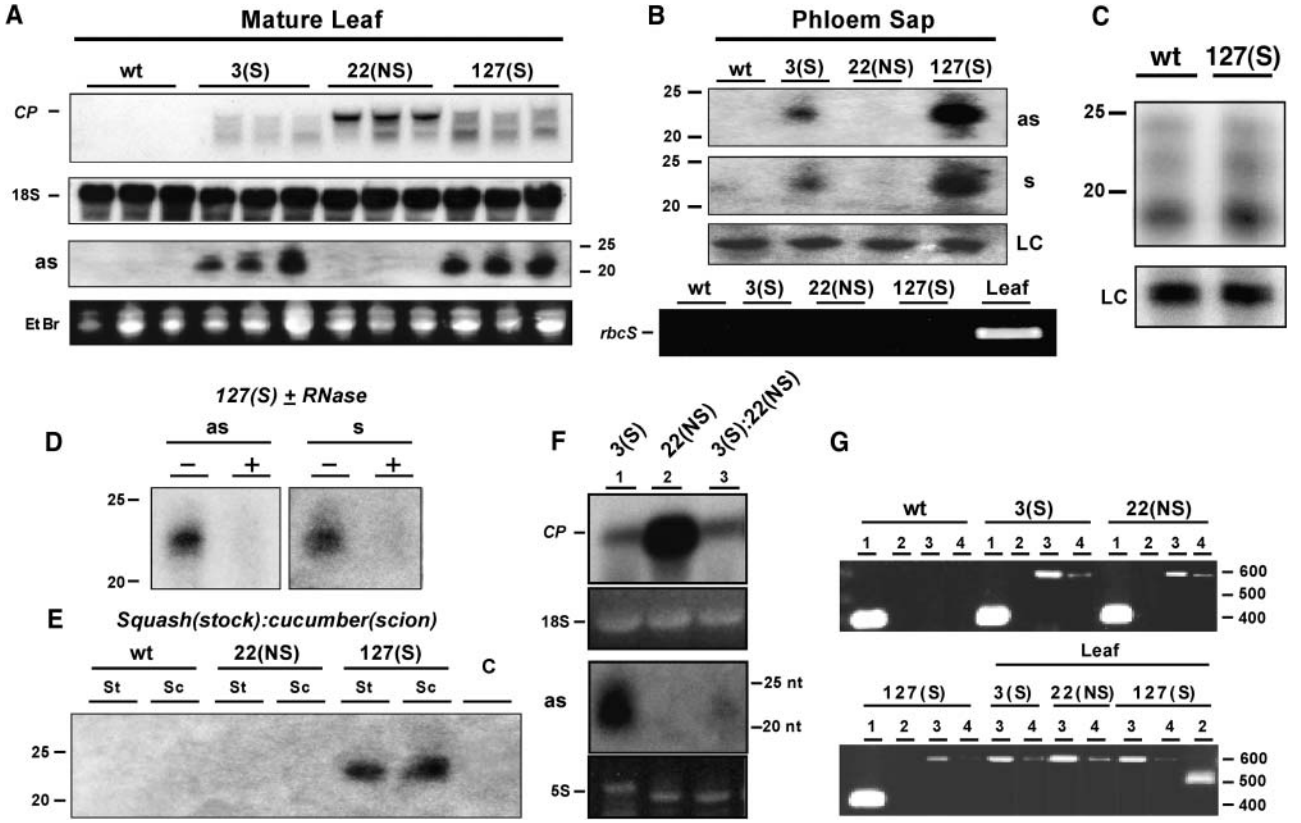

Figure 4. Identification of RNA Species in the Phloem of Spontaneously Silencing *CP* Transgenic Squash Lines.

(A) RNA gel blot analysis of RNA extracted from spontaneously silencing [3(S) and 127(S)] and nonsilencing [22(NS)] squash lines expressing the *CP* of *Squash mosaic virus* ([SqMV]; Pang et al., 2000). Top panels: hybridization analysis performed with *CP* and *18S* probes. Bottom panels: small RNA detected using antisense (as) *CP* riboprobe; loading control provided by ethidium bromide staining (EtBr).

(B) RNA gel blot analyses performed on phloem sap collected from squash lines in **(A)**, using antisense and sense (s) riboprobes. LC, loading control. Bottom panel: phloem sap integrity confirmed by RT-PCR using *rbcS* primers.

(C) Comparison of small RNA populations present in the phloem sap of wild-type and *CP* transgenic spontaneously silencing (line 127) squash plants.

(D) ssRNA-specific RNase assay.

(E) RNA gel blot analysis performed on phloem sap collected from heterografted plants, using antisense riboprobe. Positive signals were detected in phloem sap collected from both the stock (St, squash) and cucumber scion (Sc) samples taken from heterografted 127(S) plants, a spontaneously silencing line. Signal was not detected in the phloem from heterografted nonsilencing *CP* transgenic line 22(NS) nor from homografted wild-type squash or cucumber (C) plants. Equivalent results were obtained using sense riboprobe.

(F) RNA gel blot analysis of SqMV *CP* RNA (top panel) and siRNA (bottom panel) extracted from the scion apex of control [homografted 3(S) and 22(NS)] and heterografted [3(S) stock:22(S) scion] plants. Loading controls: *18S* and *5S* riboprobes.

(G) RT-PCR analysis detected sense and antisense *CP* transcripts in phloem sap collected from summer-grown squash. *CP* primers were used to amplify full-length transcripts (600 bp) from phloem sap and leaf RNA samples collected from wild-type and *CP* expressing squash lines. RT-PCR performed with internal *CP* primers gave similar results. Controls for these experiments used primers for *CmPP16* (400 bp) and *rbcS* (500 bp). Lanes are as follows: 1, *CmPP16*; 2, *rbcS*; 3, *CP* sRNA; 4, *CP* antisense RNA.

CmRINGP and using fractionated pumpkin phloem proteins is presented in Figures 6A and 6B. Equivalent experiments performed with cucumber and lupin phloem proteins are shown in Figures 7A and 7B and Figures 7F and 7G, respectively. These mRNA binding patterns were then compared with those obtained using either sense or antisense synthetic 25-nucleotide RNA. Analysis of pumpkin (Figures 6D and 6E), cucumber (Figures 7C and 7D), and lupin (Figures 7H and 7I) revealed the presence of an ~27-kD protein that bound differentially and strongly to small RNA. Parallel experiments performed using phloem-purified small RNA (18 to 24 nucleotides) from pumpkin confirmed this finding (Figure 6F). Finally, experiments conducted using various double-stranded forms of small RNA (Figures 6G to 6I) showed that the pumpkin 27-kD protein bound to both small ssRNA and dsRNA, albeit with an apparent higher affinity for ssRNA species.

Biochemical protocols were next developed to purify the pumpkin 27-kD phloem protein to permit cloning of the corresponding gene. As shown in Figure 8A, a combination of Q-Sepharose and metal-chelation chromatography yielded

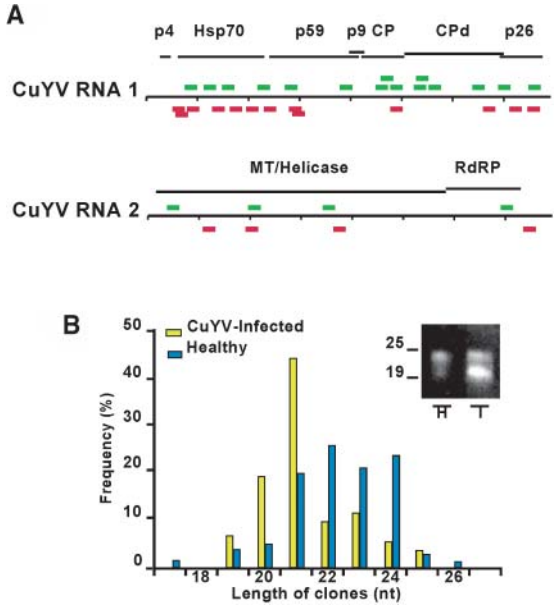

Figure 5. Identification of RNA Species in the Phloem of Virus-Infected Pumpkin Plants.

(A) Distribution of sense (green) and antisense (red) clones directed against both RNA 1 and RNA 2 of the CuYV genome. Viral open reading frames are as described (Hartono et al., 2003), and the presence of viral transcripts in the phloem sap was confirmed using standard protocols.
(B) Size distribution of clones reflected in phloem small RNA databases prepared from healthy and CuYV-infected pumpkin plants. Inset, small RNA populations present in healthy (H) and infected (I) phloem sap. Bioinformatic analysis revealed that 57% of the small RNA clones from CuYV-infected plants displayed 100% identity to this viral genome, a majority 20- to 21-nucleotide size class. Database for healthy plants lacked any clones having sequence homology to CuYV. nt, nucleotides.

a highly purified protein preparation that was used for chymotrypsin digestion, microsequencing, and mass spectroscopy. The conceptual translation of the identified gene, termed *CmPSRP1*, is presented in Figure 8B. PSRP1 has a predicted mass of 20,454 D that was consistent with the value of 21,004 D as determined by mass spectroscopic analysis of phloem-purified PSRP1. We previously reported that PSRP1 is phosphorylated by a Ca^{2+}-dependent protein kinase in vitro (Yoo et al., 2002), and this difference in molecular mass is consistent with post-translational modification.

Analysis of CmPSRP1 identified two highly repetitive sequences, HGHGPA(S)GG and CQPANPNVGH. In addition, there were 16 imperfect octapeptide (P-A/S-G/W-G-H-G-H/C-G) repeats, starting at residue 33 (P) and extending to 160 (G), and three decapeptide repeats (H-C-Q-P-A-**N/S**-P-N-V-G) from residues 166 to 196 (note that N is not conserved). DNA gel blot analysis indicated that *CmPSRP1* is a single copy gene in pumpkin (data not shown). A BLAST search of the plant databases failed to identify highly homologous genes, most probably because of the low complexity associated with PSRP1. However, analysis based on the identified repeats revealed distantly related genes in animal and plant databases. Finally, given the high His content of PSRP1, a commercial monoclonal anti-His_6 antibody was used in protein gel blot analyses of pumpkin (Figure 6C), cucumber (Figure 7E), and lupin (Figure 7J) fractionated phloem proteins. The similarity in patterns obtained by protein gel blot and RNA overlay analysis is consistent with PSRP1 being a small RNA binding protein that could be a common component of the higher plant phloem translocation stream.

PSRP1 Binds RNA in a Size- and Form-Specific Manner

Gel mobility-shift assays were next performed to further investigate the RNA binding properties of PSRP1. For these studies, both phloem-purified and recombinant (R-PSRP1; Figure 8C) forms were used and yielded equivalent results. As illustrated in Figure 9, PSRP1 exhibited both form- and size-specific RNA binding properties. Parallel gel mobility-shift experiments performed on 25-nucleotide ssRNA and 25-nucleotide dsRNA indicated that PSRP1 preferentially bound to the ssRNA form (Figure 9A). Competition experiments were next performed by preincubating PSRP1 with different concentrations of unlabeled ssRNA or dsRNA, followed by the addition of ^{32}P-labeled 25-nucleotide ssRNA (as competitor) (Figures 9B and 9C). Analysis of these data yielded PSRP1 dissociation constants (K_d) for 25-nucleotide ssRNA and 2-nucleotide 3′ 25-nucleotide dsRNA of 3.13×10^{-8} M and 3.06×10^{-5} M, respectively.

To investigate whether PSRP1 exhibits size specificity in binding to RNA, a competition series was conducted using ssRNA of various lengths. Purified R-PSRP1 was allowed to interact with different amounts of unlabeled 25-, 45–, 100-, 400-, and 1000-nucleotide ssRNA molecules. This preincubation step was followed by the addition of ^{32}P-labeled 25-nucleotide ssRNA probe. Based on these experiments, PSRP1 appears to bind preferentially to ssRNA molecules in the following order: 25 nucleotides > 45 nucleotides > 100 nucleotides = 400 nucleotides = 1000 nucleotides (Figure 9D). Taken together, our biochemical assays provided support for the hypothesis that PSRP1 functions as a phloem small RNA binding protein.

CmPSRP1 Is Expressed in Vascular Tissues

The expression pattern of *PSRP1* was next investigated using a combination of specific primers and in situ RT-PCR methods (Ruiz-Medrano et al., 1999). As illustrated in Figure 10, *PSRP1* transcripts were detected in pumpkin vascular tissues, with the highest levels accumulating in both the internal and external phloem (Figure 10B). Two forms of control were employed in these studies: one involved using primers for *CmPP16* (Xoconostle-Cázares et al., 1999) (Figure 10C), and in the other, primers were omitted from the reaction mixture (Figure 10D). The similarity between the patterns of *CmPSRP1* and *CmPP16* mRNA accumulation was fully consistent with the presence of both proteins within the pumpkin phloem sap.

PD Do Not Permit Cell-to-Cell Diffusion of Small RNA Species

By virtue of their small size, it has been assumed that small ssRNA and dsRNA move from cell to cell through PD by simple

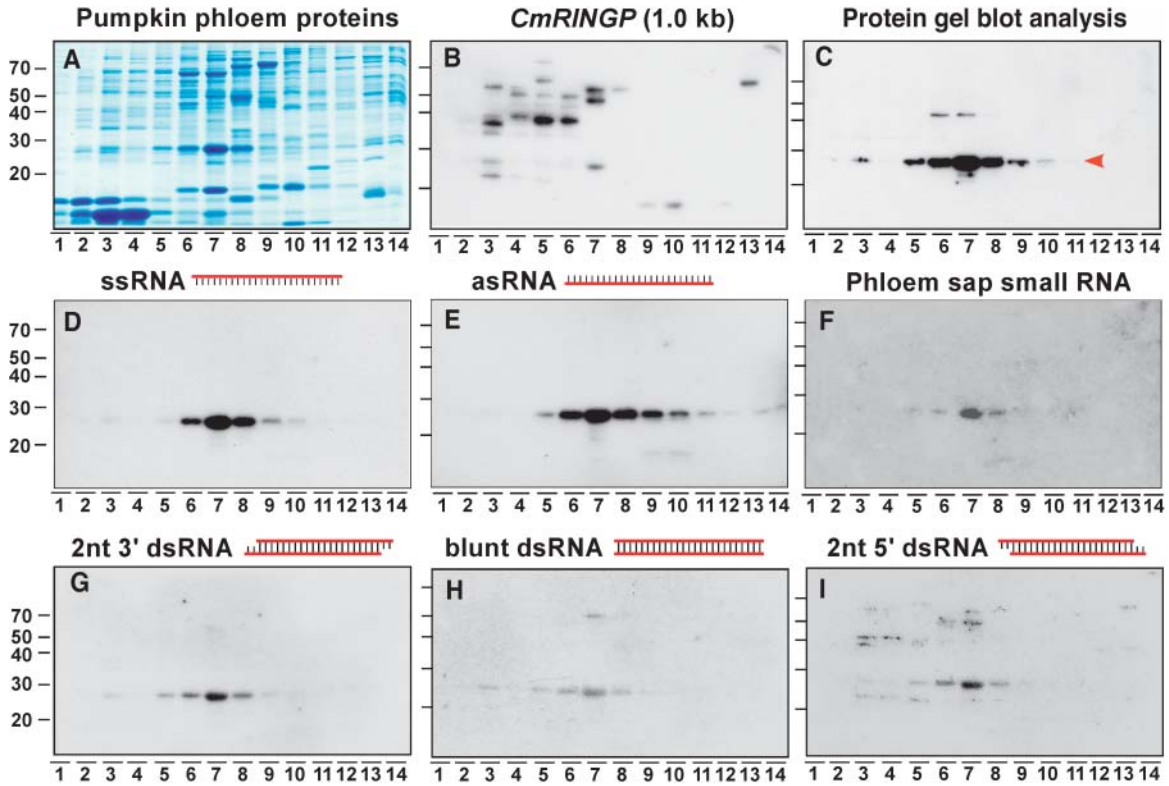

Figure 6. Identification of a Small RNA Binding Protein Present in Pumpkin Phloem Sap.

(A) Pumpkin phloem sap fast protein liquid chromatography (FPLC)-fractionated proteins.

(B) RNA overlay-protein blot assay performed on FPLC-fractionated proteins from **(A)** using a *CmRINGP*-specific riboprobe (Ruiz-Medrano et al., 1999). Note the complement of phloem RNA binding proteins (PRB) capable of recognizing this phloem-mobile mRNA.

(C) Detection of a 27-kD PRB (arrowhead) by a monoclonal anti-His_6 antibody.

(D) to **(I)** Northwestern assays performed on FPLC-fractionated phloem proteins from **(A)** using the indicated forms of small RNA riboprobes. Note that all probes bound to a 27-kD PRB.

diffusion (Mlotshwa et al., 2002). If this were the case, PSRP1 could bind to small RNA species to restrict their movement from the phloem translocation stream out into vascular cells. Microinjection techniques were employed to test whether small RNA can actually diffuse through PD. Various forms of 21- and 25-nucleotide ssRNA and dsRNA were fluorescently labeled and injected into target cells, and their movement was observed by confocal laser scanning microscopy. The results from these studies are presented in Table 2. Although small membrane impermeant fluorescent probes like LYCH could undergo extensive cell-to-cell movement, none of the small RNA species tested was observed to move out of the injected cell. Retention of these fluorescently tagged 25-nucleotide ssRNA and dsRNA probes within the target cell is illustrated in Figures 11A and 11B, respectively. Hence, the PD size exclusion limit ([SEL]; ~800 D; Robards and Lucas, 1990) in mesophyll cells appears to prevent diffusion of these small RNA molecules.

To further explore the ability of small RNA molecules to move through PD, we next used endogenous KNOTTED1 (KN1) and viral movement proteins *Cucumber mosaic virus* movement protein (CMV-MP) because they are known to mediate an increase in PD SEL during their cell-to-cell trafficking (Carrington et al., 1996; Gilbertson and Lucas, 1996; Zambryski and Crawford, 2000; Haywood et al., 2002). These studies confirmed that such movement protein trafficking potentiated the cell-to-cell diffusion of 20-kD F-dextran, but in no case did this facilitate diffusion of the coinjected small RNA (Tables 2 and 3, Figures 11C and 11D). As an additional control for these experiments, we coinjected either KN1 or CMV-MP along with Alexa fluor–labeled *CmRINGP*. Here, CMV-MP but not KN1 could mediate trafficking of this RNA molecule (Table 2). Given that the size of both the 25-nucleotide ssRNA and dsRNA (~8 and ~16 kD, respectively) is below that of the 20-kD F-dextran, and well below that of the 1-kb *CmRINGP* RNA, the observed lack of small RNA movement may reflect either sequestration within the cell or involvement of a more complex mechanism.

Selective PD Trafficking of 25-Nucleotide ssRNA Mediated by PSRP1

Our microinjection studies raised the possibility that PSRP1 could function in the cell-to-cell trafficking of small RNA. Evidence in support of such a function was gained through experiments performed with native phloem and recombinant forms of

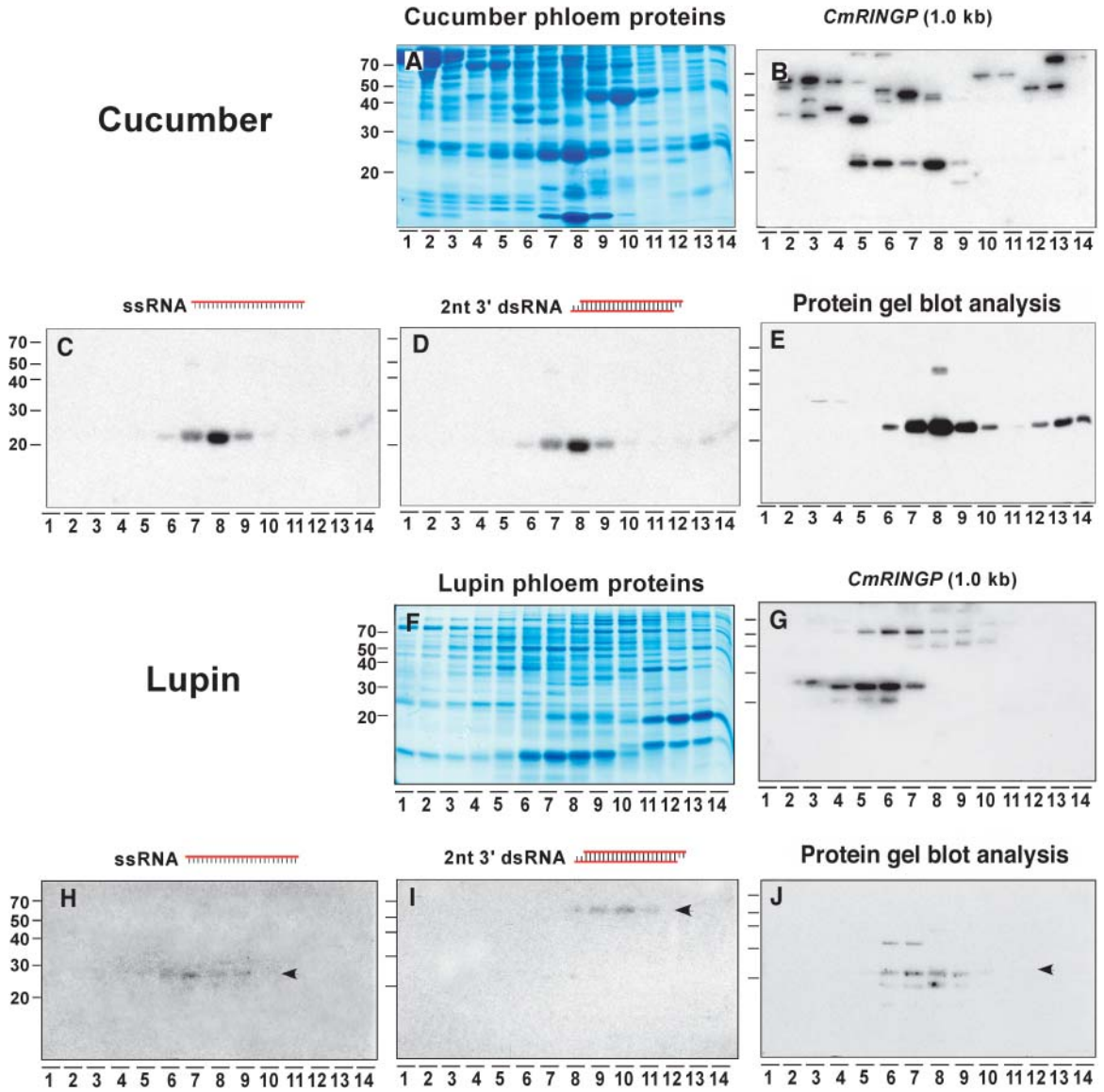

Figure 7. Identification of a Small RNA Binding Protein Present in Cucumber and Lupin Phloem Sap.

(A) Cucumber phloem sap FPLC-fractionated proteins.
(B) Northwestern assay performed on FPLC-fractionated proteins from **(A)** using a *CmRINGP*-specific riboprobe. Note the set of cucumber PRBs capable of recognizing this pumpkin phloem-mobile mRNA.
(C) and **(D)** RNA overlay-protein blot assays performed on FPLC-fractionated phloem proteins from **(A)** using the indicated forms of small RNA riboprobes. Note that both probes bound to a single PSRP1 in the 27-kD size range.
(E) Detection of a 27-kD PSRP1 by a monoclonal anti-His_6 antibody.
(F) Lupin phloem sap FPLC-fractionated proteins.
(G) RNA overlay-protein blot assay performed on FPLC-fractionated proteins from **(A)** using a *CmRINGP*-specific riboprobe. Note the set of lupin PRB capable of recognizing this pumpkin phloem-mobile mRNA.
(H) and **(I)** RNA overlay-protein blot assays performed on FPLC-fractionated phloem proteins from **(F)** using the indicated forms of small RNA riboprobes. Note that the ssRNA probe bound to a 27-kD protein, whereas the dsRNA probe bound to a 55-kD protein.
(J) Detection of a 27-kD PSRP1 by a monoclonal anti-His_6 antibody.

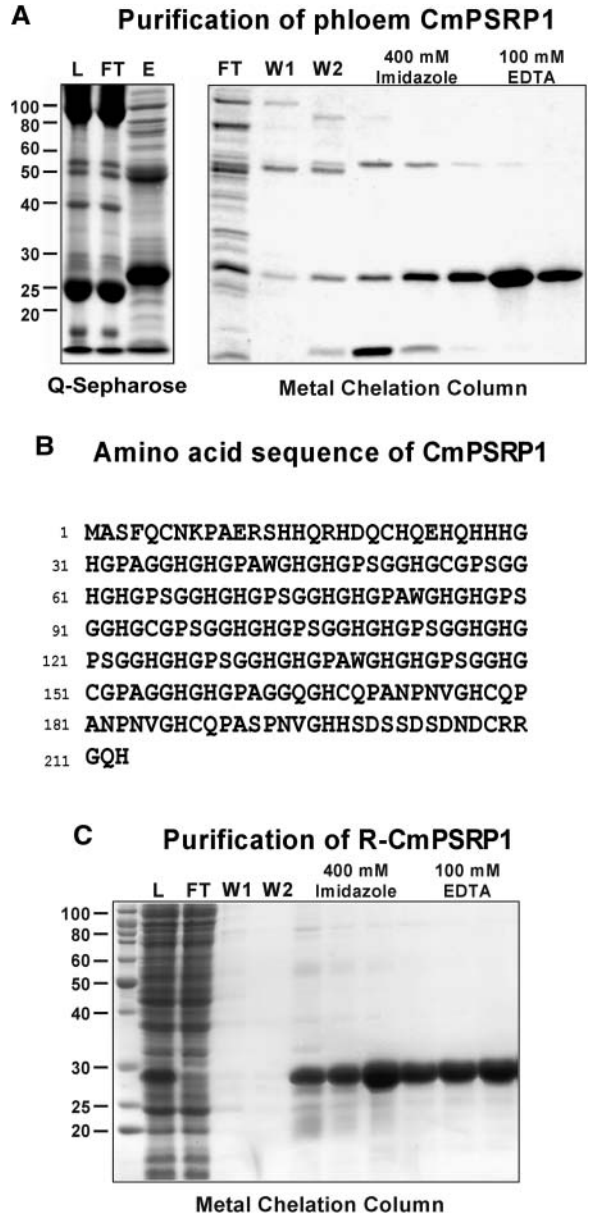

Figure 8. Purification, Cloning, and Expression of PSRP1.

(A) Purification of the 27-kD PSRP1 from pumpkin phloem sap using a combination of Q-Sepharose and metal chelation chromatography. Protein profiles contained within the anion-exchange fractions (L, loading; FT, flow-through; E, elution) were resolved by 10% SDS-PAGE (an equal volume [20 μL] was loaded for each fraction). Protein profiles for metal chelation resolved as above (FT, flow-through; W1/ 2, washes).

(B) Conceptual translation of *CmPSRP1* (GenBank accession number AY326308) yielded a 20,454-D protein. The predicted molecular mass was consistent with the value of 21,004 D as determined by mass spectroscopy with the 27-kD PSRP1 in **(A)**.

(C) Purification of recombinant (R)-PSRP1 using metal chelation chromatography. Proteins from each step were resolved by 10% SDS-PAGE and visualized using GelCode Blue.

this protein. As illustrated by the data presented in Table 3, coinjection of phloem fraction 7, containing the highest level of PSRP1 (see Figures 6A and 6C), and Alexa Fluor–labeled 25-nucleotide ssRNA resulted in trafficking into neighboring cells. Phloem fraction 10 (containing a very low level of PSRP1) was used as a control for this experiment; note that proteins contained within this fraction were unable to mediate the trafficking of the 25-nucleotide ssRNA probe. A parallel series of experiments, conducted using 25-nucleotide dsRNA as the test molecule, demonstrated that neither phloem fraction 7 nor 10 could potentiate trafficking from the target cell (Table 3).

Experiments performed with purified native phloem PSRP1 and R-PSRP1 demonstrated that both forms were able to mediate the cell-to-cell movement of a 25-nucleotide ssRNA probe. During this trafficking event, the PD SEL was increased to >20 kD. Coinjection of R-PSRP1, 20-kD F-dextran and Alexa Fluor (568)–labeled 25-nucleotide ssRNA resulted in efficient movement of both fluorescent signals into the adjoining cells (Table 3, Figures 11E and 11F). Again, this PSRP1 movement capacity appeared to be specific to small ssRNA because it failed to traffic large RNA transcripts (e.g., *CmRINGP*), small dsRNA, and ssDNA (Table 3, Figures 11G and 11H). Coinjection of BSA with 25-nucleotide ssRNA or ssDNA did not result in trafficking of either probe; this provided an essential test for possible nonspecific effects that might have been associated with injection of protein, per se, into the target cell.

DISCUSSION

Small RNA Population in Phloem Sap

Our findings support the hypothesis that the phloem translocation stream contains both a small RNA binding protein and a seemingly complex population of small RNA molecules that are responsive to growth conditions, as well as to viral challenge. In contrast with the apex, the phloem of cucurbits appears to contain three discrete small RNA size classes. In summer-grown plants, the relative abundance of each size class appeared to vary as a function of position along the plant axis; however, a more uniform pattern was observed in plants grown under winter conditions. Castor bean phloem contained only one major small RNA band, whereas those of lupin and yucca exhibited a greater diversity in size (Figure 1). In vitro studies have also indicated that plants can produce a range of small RNA species (Tang et al., 2003), and in this study it was concluded that such size variation in si/miRNA probably reflected the involvement of different DCL enzymes. Given the similarity in molecular size distribution obtained in our study (Figure 2A) and that reported by Tang et al. (2003), the observed phloem si/miRNA populations might similarly reflect the involvement of several DCLs. Differences in small RNA profiles contained within samples from the apex and pumpkin phloem sap presumably reflect the action of specific DCL enzymes located in these tissues.

Authentication of Phloem Small RNA Population

Our biochemical and bioinformatic studies provided support for the conclusion that small RNA molecules, extracted from the

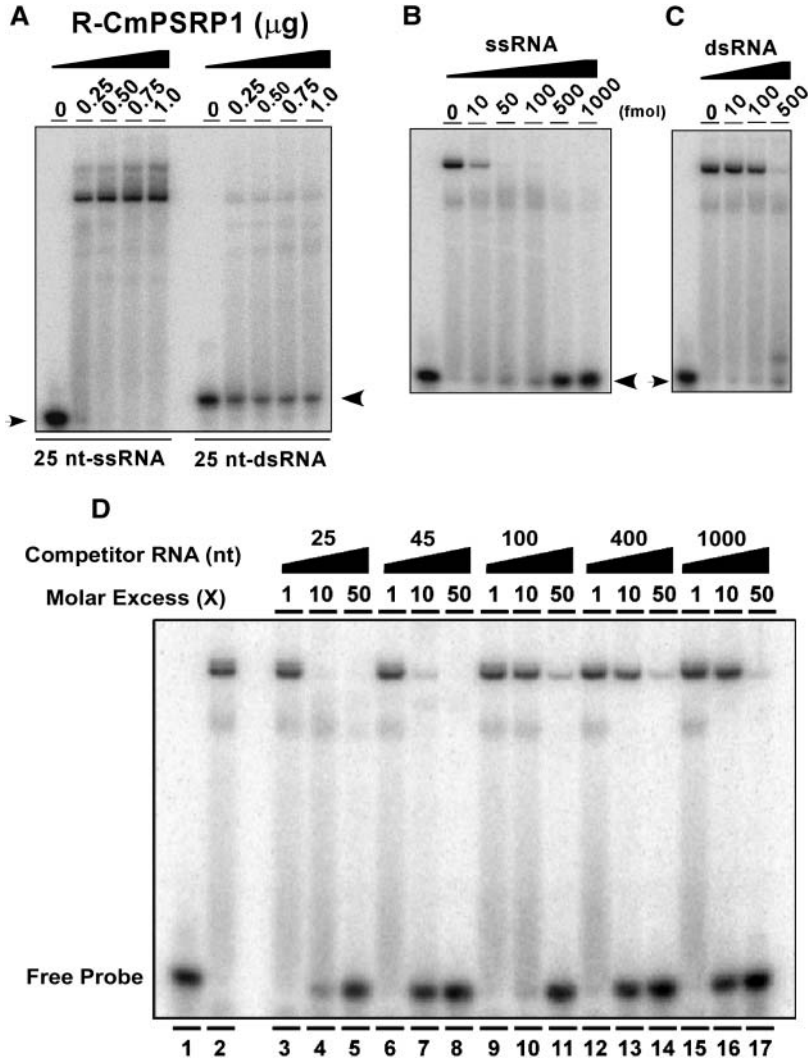

Figure 9. Recombinant PSRP1 Displayed Form- and Size-Specific RNA Binding Properties.

(A) Gel mobility-shift assays performed using R-PSRP1 and ssRNA and dsRNA probes (10 fmol). nt, nucleotides.

(B) and **(C)** Competition experiments performed by preincubating R-PSRP1 (0.25 μg) with different concentrations of unlabeled ssRNA or dsRNA, respectively, followed by competition with ^{32}P-labeled 25-nucleotide ssRNA (10 fmol). R-PSRP1 dissociation constants (K_d) for 25-nucleotide ssRNA and 2-nucleotide 3′ 25-nucleotide dsRNA were 3.13×10^{-8} M and 3.06×10^{-5} M, respectively.

(D) Competition experiments performed with ssRNA of various lengths. Purified R-PSRP1 (0.2 μg) was mixed with different amounts (molar excess indicated) of unlabeled 25-nucleotide (lanes 3 to 5), 45-nucleotide (lanes 6 to 8), 100-nucleotide (lanes 9 to 11), 400-nucleotide (lanes 12 to 14), or 1000-nucleotide (lanes 15 to 17) ssRNA molecules, followed by addition of radioactively labeled 25-nucleotide ssRNA (10 fmol) probe. Complexes were analyzed by 5% PAGE. Lane 1, free probe only; lane 2, probe with R-PSRP1 only. Different length for each competitor RNA was taken into account in calculating the molar excess concentration. Note that R-PSRP1 bound preferentially to ssRNA molecules in the following order: 25 nucleotides > 45 nucleotides > 100 nucleotides = 400 nucleotides = 1000 nucleotides.

cucurbit phloem sap, are bone fide products of DCL action. The complexity reflected in the phloem small RNA database is to be expected, given that RNAi directed against each target RNA would yield a highly diverse population of individual siRNA molecules. The lack of a cucurbit genome database complicated our efforts to confirm the identity of potential RNAi targets of this phloem small RNA population. In any event, our goal was to establish whether these small RNA species were consistent with systemic gene silencing. Identification of both sense and antisense small RNAs, targeted against specific transcripts, supported this notion (Figure 2C). The examples presented for the cucurbit *TnL1* and *TnL2* are fully consistent with the operation of systemic RNAi, the function of which would be to control transposon action (Wassenegger, 2002; Rudenko et al., 2003), on a whole plant level. Localized siRNA target sites were detected for several potential transcripts, including *MT*, *End*, and *Hel*

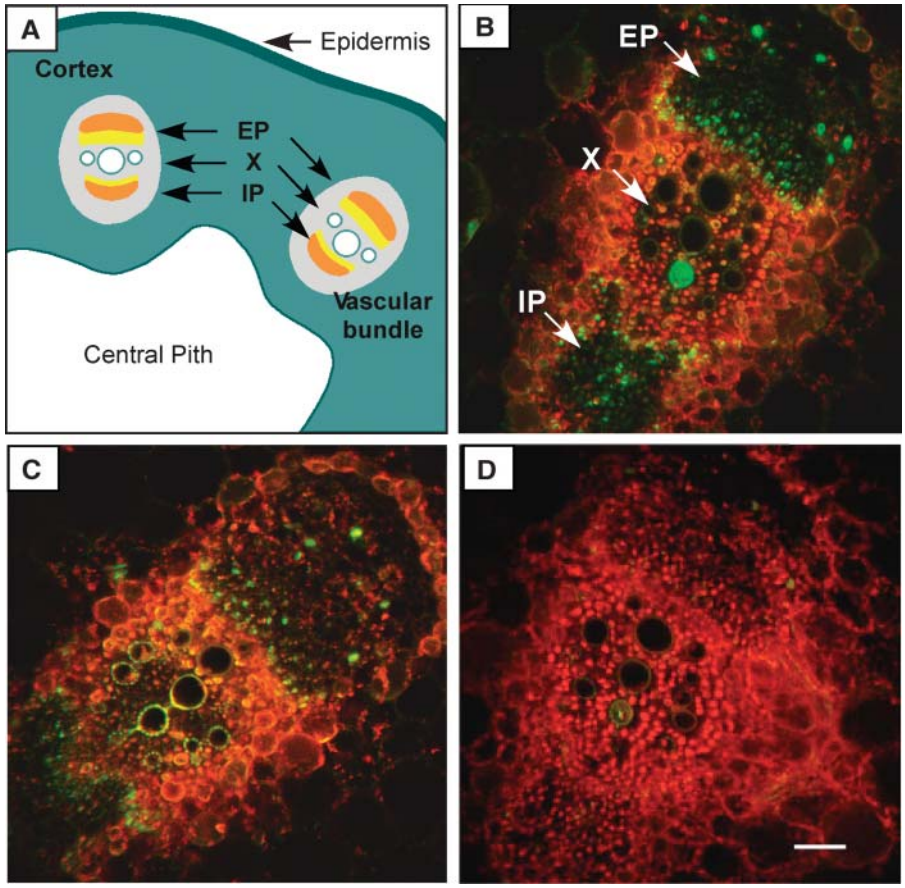

Figure 10. In Situ RT-PCR–Based Detection of *CmPSRP1* Transcripts in the Vascular System.

(A) Schematic transverse section of a portion of the pumpkin petiole. Vascular bundles are comprised of internal and external phloem (IP and EP, respectively) and xylem (X), with an intervening cambium (yellow).
(B) Confocal laser scanning microscopy image of a pumpkin petiole (transverse section) demonstrating the presence of *CmPSRP1* RNA (green signal represents incorporation of Alexa Fluor–labeled nucleotides) in phloem cells.
(C) Equivalent cellular pattern detected for *CmPP16* (Xoconostle-Cázares et al., 1999).
(D) Negative control in which primers were omitted from the RT-PCR reaction mixture. Red fluorescence represents tissue autofluorescence, and the green signal associated with the xylem reflects residual nonspecific binding of unincorporated Alexa Fluor–labeled nucleotides. Bar in **(D)** = 100 μm, common to **(B)** and **(C)**.

(Figure 2C), and this phenomenon could reflect a variation on miRNA-directed mRNA cleavage/gene regulation (Llave et al., 2002a; Carrington and Ambros, 2003; Palatnik et al., 2003).

In plants, miRNAs are thought to function through the RNAi pathway (Tang et al., 2003), where they exert control over developmental events (Llave et al., 2002a; Reinhart et al., 2002; Aukerman and Sakai, 2003; Bartel and Bartel, 2003; Kasschau et al., 2003; Kidner and Martienssen, 2003). Furthermore, miRNA molecules and the complementary sites within their targets display a high degree of conservation between species (Kidner and Martienssen, 2003; Lewis et al., 2003). These properties offered a powerful way to verify the authenticity of the phloem small RNA species because we could search the database for the presence of known miRNAs (Llave et al., 2002b; Reinhart et al., 2002; Rhoades et al., 2002). Detection of miR156, miR159, and miR167 (Figure 2C, Table 1), as examples, supported our notion that small RNAs in phloem sap represent a bone fide population of si/miRNA derived from the phloem translocation stream. RNA gel blot analysis performed with these miRNAs provided additional verification (Figure 3); all three miRNAs were detected to varying levels in the tissues analyzed, but the strongest signal was generally observed in the phloem sap. Here, it is noteworthy that miR171, which targets the *Scarecrow-like* gene family in Arabidopsis (Llave et al., 2002a), was absent from the phloem database and undetectable in phloem sap. Taken together, these results indicate that the si/miRNA population within the cucurbit phloem can provide a platform to investigate systemic gene silencing in plants.

Systemic Activity of Transgene-Derived siRNA

Transgenic squash lines expressing a viral *CP* gene provided an important test for the concept that systemic silencing occurs

Table 2. Small RNA Species Are Unable to Move Cell to Cell through Undilated or Dilated Plasmodesmal Microchannels

	Microinjection	
Injected Material[a]	Total (*n*)	Movement [*n* (%)][b]
LYCH	10	10 (100)
FITC-dextran (20 kD)	30	3 (10)
21-nt ssRNA	10	0 (0)
25-nt ssRNA	35	0 (0)
25-nt dsRNA (blunt ended)	10	0 (0)
25-nt dsRNA (2-nt 3′ overhang)	8	0 (0)
25-nt dsRNA (2-nt 5′ overhang)	8	0 (0)
21- to 25-nt dsRNA (4-nt 3′ overhang)	10	0 (0)
R-KN1[c] + 20-kD FITC-dextran	26	24 (96)[d]
R-KN1 + *CmRlNGP* RNA (sense, 1 kb)	12	0 (0)
R-KN1 + 25-nt ssRNA	6	0 (0)
R-KN1 + 20-kD FITC-dextran + 25-nt ssRNA	5	5/0 (100/0)[e]
R-CMV-MP[c] + FITC-dextran (20 kD)	10	10 (100)
R-CMV-MP + *CmRlNGP* RNA (sense, 1 kb)	10	10 (100)
R-CMV-MP + 25-nt ssRNA	10	0 (0)
R-CMV-MP + FITC-dextran (20 kD) + 25-nt ssRNA	13	13/0 (100/0)[f]
R-CMV-MP + FITC-dextran (20 kD) + 25-nt dsRNA	13	12/0 (92/0)[f]

[a] Fluorescent probes were as follows: LYCH, lucifer yellow CH; FITC-dextran, fluorescein isothiocyanate–labeled dextran; RNA probes, Alexa Fluor 568 (red) or 488 (green) labeled and injected at 1-μg/μL concentration. nt, nucleotides.

[b] Number of injections, and percentage of total injections, in which probe moved from the target cell.

[c] Recombinant (R)-KN1 and R-CMV-MP were expressed in *E. coli*, purified, and used in microinjection studies at 1.5 μg/μL.

[d] Control condition in which probe moved radially out through four to five cells.

[e] Coinjection experiments in which R-KN1/R-CMV-MP potentiated extensive trafficking of 20-kD FITC-dextran but not Alexa Fluor 568–labeled 25-nucleotide ssRNA.

[f] Movement of the RNA probe (or 20-kD FITC-dextran) was restricted to neighboring cells, and the small RNA signal very often accumulated in their nuclei.

through phloem-mediated delivery of siRNA species. The presence of *CP* siRNA in phloem sap collected from spontaneously silencing plants [lines 3(S) and 127(S)], but its absence from nonsilencing plants [line 22(NS)] (Figures 4A and 4B), was fully consistent with this systemic silencing hypothesis and the observed resistance to SqMV (Pang et al., 2000). It is worth noting that when expression was driven by a strong promoter, these *CP*-derived 23-nucleotide siRNA still seemed to represent only a minor component of the squash phloem small RNA population (Figure 4C). This finding is in marked contrast with the situation in which 57% of the clones analyzed from phloem sap derived from CuYV-infected plants exhibited 100% identity to the viral genome (Figure 5). Thus, the level of siRNA in the phloem sap probably reflects the level of mRNA and RNA-dependent RNA polymerase plus DCL activities within companion cells.

Heterografting experiments performed between spontaneously silencing squash (stock) and wild-type cucumber (scion) plants provided direct proof that *CP* siRNA can enter and move with the phloem translocation stream (Figure 4E). Excision of each scion from its stock means that sap cannot be contaminated with RNA that might otherwise be released from stock companion cells during sap collection. Hence, detection of *CP* siRNA, in the cucumber scion sap, further supports the concept that siRNA is a bone fide component of the phloem translocation stream. Our observation that *CP* silencing occurred in the apical tissues of the nonsilencing line 22(NS), when line 3(S) served as the stock (Figure 4F), is also consistent with *CP* siRNA delivery and activation of RNAi.

An unexpected finding from our studies with phloem sap derived from *CP* transgenic squash lines was the fact that, using RT-PCR, we could detect full-length sense and antisense *CP* transcripts (Figure 4G). The presence of *CP* sense RNA in the phloem sap of lines 3(S), 127(S), and 22(NS) might reflect properties associated with viral movement, which would account for its presence in all lines tested. Because high transcript levels can trigger primer-independent RNA-dependent RNA polymerase–mediated synthesis of complementary RNA (cRNA) (Tang et al., 2003), the level of *CP* RNA in companion cells of all three lines might have been sufficient to activate *CP* cRNA production. In this scenario, the presence of *CP* cRNA might reflect contamination from the surrounding tissues because only a weak signal could be amplified with phloem sap collected from all plant lines. However, this possibility is at variance with our controls that confirmed the integrity of the collected phloem sap (Figure 4G).

A further point of note is that the presence of low levels of sense and antisense *CP* RNA in the phloem of line 22(NS) did not induce silencing in the homograft combination; this result is consistent with *CP* 23-nucleotide siRNA acting as the silencing signal. Molecular analysis of phloem sap collected from CuYV-infected pumpkin (Figure 5) similarly provided support for the hypothesis that systemic RNAi involves a combination of sense and antisense siRNA. In any event, detection of sense and antisense siRNA (from *CP* transcripts or the CuYV genome) in the long-distance translocation stream suggests that these molecules probably serve as one component of the systemic silencing system (Jorgensen et al., 1998; Lucas et al., 2001; Vance and Vaucheret, 2001; Mlotshwa et al., 2002). Given that the *CP* and CuYV siRNA were in the 23-nucleotide and 21-nucleotide size range, respectively, it would seem that transmission of systemic silencing does not involve a specific size class (Mallory et al., 2001, 2003; Vance and Vaucheret, 2001; Hamilton et al., 2002; Klahre et al., 2002; Mlotshwa et al., 2002; Himber et al., 2003); therefore, the process probably reflects the operation of a range of DCL systems.

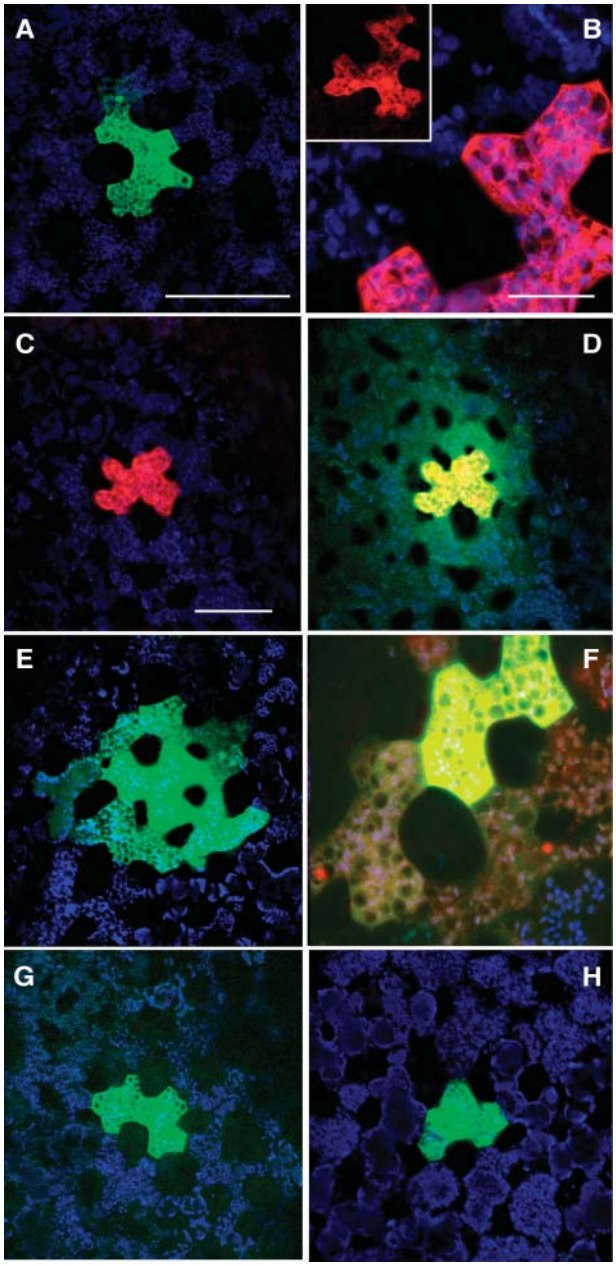

Figure 11. PSRP1 Can Mediate Form-Specific Cell-to-Cell Movement of Small RNA.

(A) and **(B)** Retention in the target cell of microinjected fluorescently labeled synthetic 25-nucleotide ssRNA **(A)** or dsRNA **(B)**. Inset shows low-magnification image of entire cell.

(C) and **(D)** Cell-to-cell trafficking of KN1 through PD potentiated extensive movement of FITC-labeled 20-kD dextran (**[D]**, green signal), but the coinjected 25-nucleotide ssRNA (red signal) was unable to diffuse out of the target cell **(C)**.

(E) Phloem-purified CmPSRP1 mediated cell-to-cell movement of co-injected fluorescently labeled (green) 25-nucleotide ssRNA.

(F) Equivalent experiment to that presented in **(E)**, demonstrating movement of both 20-kD dextran (green) and 25-nucleotide ssRNA (red). Note the confinement of the fluorescent signals to neighboring cells (**[E]** and **[F]**).

(G) and **(H)** Neither 25-nucleotide dsRNA **(G)** nor 25-nucleotide ssDNA **(H)** moved from the target cell when coinjected with phloem-purified CmPSRP1. All images were collected by confocal microscopy 20 min after injection into mesophyll cells in mature leaves of *Nicotiana benthamiana*. Bars = 100 μm; **(C)** common to **(D)** to **(H)**.

PSRP1: A Phloem Small RNA Binding Protein

The phloem of pumpkin, cucumber, and lupin contains a diverse population of proteins having the capacity to bind RNA. Pumpkin proteins that bind to phloem-mobile transcripts, such as *CmRINGP* (Ruiz-Medrano et al., 1999), do not appear to recognize small RNA species (Figure 6). Although the actual proteins involved were different, we observed a similar RNA binding capacity with FPLC-fractionated phloem protein from cucumber and lupin. The converse appeared to hold, in that PSRP1, a phloem protein that migrates in the 27-kD region on SDS-PAGE, was shown to bind specifically to small ssRNA and dsRNA, but not to the 1-kb RNA of *CmRINGP*. Putative PSRP1 orthologs in cucumber and lupin displayed quite similar binding specificity, except that in lupin this phloem protein did not appear to bind small dsRNA (Figure 7I). However, rather than a difference in binding properties, this situation may well reflect the lower level of total protein that could be collected from lupin phloem sap.

Considering the evolutionary divergence between these species, this similarity in protein binding pattern with small RNA suggests a high level of conservation in terms of the function of the encoding genes. Protein gel blot analysis also provided support for this hypothesis, in that a commercial anti-His_6 antibody displayed a high level of specificity in that it basically reacted only with the small RNA binding protein present in the phloem sap from each of the species analyzed (Figures 6C, 7E, and 7J). Additional weight is afforded this observation when one considers the overall complexity in the protein profiles associated with each phloem translocation stream (Figures 6A, 7A, and 7F).

The low complexity associated with the PSRP1 predicted amino acid sequence (Figure 8B) confounded our search for related genes in other species. A general screen for PSRP1 orthologs might be developed based on their predicted small RNA binding properties. Proteins derived from expression of vascular-based libraries (Figure 10C demonstrates the pattern of *CmPSRP1* mRNA accumulation in the phloem) could be used in RNA overlay experiments. The feasibility of this approach is strengthened by the fact that, in pumpkin, *PSRP1* is a single gene family.

PSRP1 Selectively Binds and Mediates Small ssRNA Trafficking

The phloem sap of squash lines 3(S) and 127(S) contained nearly equal levels of sense and antisense siRNA (Figure 4B). Our RNase assays suggested that these *CP*-derived siRNA are present in the phloem as ssRNA species, as opposed to double-stranded duplexes (Figure 4D). A similar conclusion

Table 3. PSRP1 Mediates Form-Specific Cell-to-Cell Movement of Small RNA

	Microinjection	
Injected Material[a]	Total (*n*)	Movement [*n* (%)][b]
Phloem fraction 7[c] + 25-nt ssRNA	13	8 (62)[d]
Phloem fraction 10 + 25-nt ssRNA	8	1 (13)
Phloem fraction 7 + 25-nt dsRNA (blunt)	10	0 (0)
Phloem fraction 10 + 25-nt dsRNA (blunt)	9	1 (11)
Phloem-purified PSRP1 + 25-nt ssRNA	6	5 (83)[d]
R-PSRP1[c] + 25-nt ssRNA	26	20 (80)[d]
R-PSRP1 + 20-kD FITC-dextran	11	11 (100)[d]
R-PSRP1 + 20-kD FITC-dextran + 25-nt ssRNA	5	5/5 (100/100)[d]
R-PSRP1 + *CmRINGP* RNA (1 kb)	8	0 (0)
R-PSRP1 + 25-nt dsRNA (2-nt 3′ overhang)	5	0 (0)
R-PSRP1 + 25-nt ssDNA	14	0 (0)
BSA + 25-nt ssRNA	8	0 (0)
BSA + 25-nt ssDNA	8	0 (0)

[a] Fluorescent probes were as follows: FITC-dextran and RNA probes Alexa Fluor 568 (red) or 488 (green) labeled and injected at 1-μg/μL concentration.

[b] Number of injections, and percentage of total injections, in which probe moved from the target cell.

[c] Recombinant (R)-PSRP1 was expressed in *E. coli*, purified, and used in microinjection studies at 1.5 μg/μL. Phloem protein fractions 7 and 10 were used at 0.1 μg/μL.

[d] Movement of the RNA probe (or 20-kD FITC-dextran) was restricted to neighboring cells, and the small RNA signal very often accumulated in their nuclei.

was drawn with respect to the endogenous population of small RNA species (Figure 1C). Such observations are consistent with the functional properties displayed by PSRP1, in that it exhibits selectivity in terms of the form and size of RNA to which it binds (Figure 9). The 1000-fold difference in PSRP1 binding to 25-nucleotide ssRNA compared with 25-nucleotide dsRNA (Figures 9A to 9C) would allow it to form ribonucleoprotein complexes with the small ssRNA present in the phloem translocation stream. The higher level of PSRP1 binding to 25- and 45-nucleotide siRNA over 100-, 400-, and 1000-nucleotide species is also consistent with our assays conducted on the phloem sap (Figure 6). Taken together, these results suggest that PSRP1functions in the systemic silencing pathway through its capacity to bind and form stable complexes with si/miRNA.

Microinjection experiments provided further insights into the role PSRP1 probably plays during systemic RNAi. In contrast with viral MPs and many endogenous non-cell-autonomous proteins (Lucas et al., 1995; Carrington et al., 1996; Gilbertson and Lucas, 1996; Zambryski and Crawford, 2000), PSRP1 displays a rather unique functional characteristic, in that it mediates cell-to-cell trafficking of small ssRNA one cell layer at a time (Figure 11, Tables 1 and 2). This finding is of interest in the context of recent results obtained on SHORT ROOT (Nakajima et al., 2001) and CAPRICE (Wada et al., 2002; Schiefelbein, 2003), two Arabidopsis non-cell-autonomous proteins that also undergo limited cell-to-cell movement. Mediating movement of small ssRNA across one cell boundary would be fully consistent with the cellular context of the phloem companion cell–sieve element complex in which PSRP1 would operate. However, the possibility cannot be discounted that expression in phloem tissues may permit a greater level of cell-to-cell trafficking compared with what we observed in our microinjection assays. In any event, PSRP1 may function as a shuttle system to exchange small ssRNA between companion cells and the sieve tube system.

Lastly, because small RNA molecules do not appear to be able to move unaided between cells, nor through dilated PD microchannels (Tables 1 and 2, Figure 11), our studies implicate the involvement of additional small RNA binding proteins required for local transmission of RNAi. Here, it is interesting to note that a viral suppressor of RNAi (Voinnet et al., 1999), the 19-kD protein (p19) of the tombusviruses, has been shown to bind selectively and with very high affinity to 21-nucleotide ds/siRNAs (Silhavy et al., 2002; Vargason et al., 2003; Ye et al., 2003). This p19–siRNA interaction would probably prevent the local propagation of RNAi. Given the involvement of siRNAs and miRNAs in an ever increasing number of plant processes, it will be interesting to see whether plants have evolved a parallel system to the viral p19 to regulate cell-to-cell spread of these signaling agents.

Our identification and functional characterization of the PSRP1 class of phloem RNA binding proteins provides insight into the molecular machinery involved in systemic si/miRNA signaling. These findings now establish a foundation for further dissection of the pathways and mechanisms used to exert long-distance control over viral infection, transposon activities, and transcriptional/translational processes (Dalmay et al., 2000, 2001; Fagard and Vaucheret, 2000; Vance and Vaucheret, 2001; Foster et al., 2002; Llave et al., 2002a; Mlotshwa et al., 2002; Reinhart et al., 2002; Volpe et al., 2002).

METHODS

Plant Materials

Cucurbita maxima cv Big Max (pumpkin), *Cucumis sativus* cv Straight Eight (cucumber), and *Ricinus communis* (castor bean) plants were grown in a special insect- and pathogen-free greenhouse under natural daylight conditions (summer: midday irradiance, 1200 to 1500 μmol m^{-2} s^{-1} photosynthetically active radiation [PAR], 35/20°C day/night temperatures, daylength 16 h; winter: midday PAR 800 μmol m^{-2} min^{-1}, 30/20°C day/night temperatures, daylength 12 h, extended by 300 μmol m^{-2} s^{-1} artificial PAR). Nutrients were delivered daily as described (http://greenhouse.ucdavis.edu/materials/nutrients_soil.htm). *Lupinus albus* cv 1234 (white lupin) plants were grown, during the winter/spring of 2003, in the Agronomy and Range Science field station at the University of California, Davis.

Grafting Protocols

Heterografting experiments were performed as previously described (Ruiz-Medrano et al., 1999) with modifications. Heterografts were generated between scions, cut from 6- to 8-week-old cucumber plants (vegetative apex to 2nd mature leaf) and stocks, provided by 8- to 12-week-old squash plants; inclusion of mature leaves on the scions increased grafting efficiency to >90%. Each excised scion (15 to 20 cm in length) was carefully inserted into an incision made in the main stem of the stock. The graft site was fastened and sealed with Parafilm, and the scion was then covered with a clear plastic bag that was removed 1 week later. These grafting experiments were performed under winter greenhouse conditions and involved a minimum of three independent replicates (four to five heterografts per replicate). Plants were employed for phloem sap analysis 3 weeks after grafting. Larger leaves on the scion were removed 3 d before phloem sap collection.

Phloem Sap Collection for Analysis of RNA and Proteins

Phloem sap was collected from well-watered plants, as previously described (Ruiz-Medrano et al., 1999; Yoo et al., 2002) with modifications. Briefly, stems or petioles for cucurbits, or inflorescent stalks for lupin (Atkins, 1999), castor bean (Jeschke and Pate, 1991), and yucca, were excised with a sterile razor blade and the cut surface blotted, several times, with sterile filter paper (3 MM; Whatman, Maidstone, UK). Phloem sap exuded thereafter was collected using sterile micropipette tips (200 μL) and immediately mixed either with an equal volume of protein sap collection buffer (100 mM Tris, pH 7.5, 10 mM EDTA, 5 mM EGTA, 10% [v/v] glycerol, 1% [v/v] 2-mercaptoethanol, and protease inhibitors [Complete; Roche, Indianapolis, IN]) or 200 μL with 500 μL of TRIzol reagent (Invitrogen, Carlsbad, CA) for phloem sap RNA extraction. For library construction and RNA gel blot analyses, phloem sap was collected directly into an equal volume of TRIzol. All buffers and samples were kept on ice during phloem sap collection.

Phloem RNA Quantitation

High and low molecular weight phloem RNA were separated as described below. Each sample was treated with DNase I (Invitrogen) for 15 min at 20°C, to remove any DNA that might have been released into the phloem sap, during exudate collection from sieve tube mitochondria or plastids (Knoblauch and van Bel, 1998). Phenol/chloroform extraction and ethanol precipitation were next used to obtain phloem RNA. The concentration of high molecular weight RNA was measured using the RiboGreen RNA quantitation kit (Molecular Probes, Eugene, OR) according to the manufacturer's instructions. Using these methods, pumpkin and cucumber had measured RNA levels of 300 and 400 ng of RNA/mL phloem sap, respectively.

Small RNA Analysis

Phloem sap was collected as described above. For end labeling, 200 μL of phloem sap was added to 500 μL of TRIzol reagent, and 200 μL of chloroform was then added and the sample was vortexed, followed by centrifugation (16,000*g*) for 15 min at 4°C. RNA was then precipitated (1 volume isopropanol, 1/10 volume 3 M sodium acetate, and 20 μg/mL of linear acrylamide [Ambion, Austin, TX]) overnight at −20°C, followed by centrifugation (16,000*g*) for 30 min at 4°C. The RNA pellet was washed with 80% (v/v) ethanol and resuspended in 10 μL of diethyl pyrocarbonate (DEPC)-treated water. RNA was 5′ exchange end labeled for 30 min at 37°C as described (Sambrook et al., 1989), using 10 units of T4 polynucleotide kinase (New England Biolabs, Beverly, MA) with the supplied buffer to which was added 100 μM ADP, 2.5 nM ATP, and 165 nM [γ-^{32}P]ATP (10 μCi/μL). Unincorporated ^{32}P-label was removed using a MicroSpin G-25 column (Amersham Biosciences, Piscataway, NJ) according to the manufacturer's instructions. For RNA analysis, an equal volume of Loading Buffer II (Ambion) was added and the sample heated at 95°C for 5 min, followed by electrophoresis (7 M urea/15% PAGE gel; 1-mm thickness, 15-cm length) at 300 V for ~2 h, using 1× TBE (90 mM Tris-borate and 2 mM EDTA) as running buffer. Gels were then exposed for autoradiography (Biomax MS film; Eastman Kodak, Rochester, NY). Because the overall pattern of the phloem sap RNA was observed to be quite constant from sample to sample, one band in this profile was employed as a loading control for the analysis of small RNA species.

Isolation of low molecular weight phloem sap RNA from polyacrylamide gels was performed as follows. RNA was resuspended in a total of 30 μL of DEPC-treated water and electrophoretically separated by denaturing PAGE (7 M urea/15% PAGE); small RNA was visualized by ethidium bromide staining. The region containing the 18- to 25-nucleotide RNA was excised and purified. Isolation and enrichment of small RNA extracted from leaves, apices, and stems was as described (Di Serio et al., 2001). Total RNA was extracted with TRIzol reagent, and a 50-μg aliquot was size fractionated (RNeasy mini column; Qiagen, Valencia, CA). The small RNA present in the flow-through was precipitated, as above, and the pellet washed with 80% ethanol and then resuspended in 10 μL of RNase-free water. The concentration of small RNA in the phloem sap was determined as described above for high molecular weight RNA. The values for pumpkin were in the range of 0.3 to 6.0 fmol small RNA/μL phloem sap.

Structural Analysis of Phloem Small RNA

The 5′-terminal residue of the phloem small RNA was examined using the following protocols. Aliquots (100 to 500 ng) of small RNA (both a 24-nucleotide synthetic RNA oligonucleotide and a gel-purified 18- to 25-nucleotide phloem sap RNA) were treated with 1 unit of shrimp alkaline phosphatase (Roche, Mannheim, Germany) using the supplied buffer. After enzymatic treatment, these small RNAs were separated, as described above, and analyzed for changes in electrophoretic mobility during denaturing PAGE. Self-ligation reactions were performed using 20 units of RNA ligase (Amersham Biosciences) with the supplied buffer to determine the capacity of low molecular weight phloem sap RNA to circularize and form concatemers.

Synthetic Small RNA

Chemically synthesized, deprotected, and HPLC-purified 25-nucleotide RNA oligonucleotides were obtained from Integrated DNA Technologies (Coralville, IA). Oligonucleotides used in experiments included FK202, 5′-rCrArGrUrGrUrCrUrUrCrUrCrCrCrUrCrArCrUrG-3′; FK203, 5′-rCrArGrUrGrUrCrUrUrCrUrCrCrCrUrCrArCrUrGrCrUrArCrU-3′; FK216, 5′-rGrCrArGrUrGrArGrGrGrArGrArArGrArCrACrUrG-3′; FK221, 5′-rGrGrArArArArCrUrArCrCrUrGrUrUrCrCrArUrGrGrCrCrArA-3′; FK222, 5′-rUrGrUrUrGrGrCrCrArUrGrGrArArCrArGrGrUrArGrUrUrUrU-3′; FK223, 5′-rUrUrGrGrCrCrArUrGrGrAArCrArGrGrUrArGrUrUrUrUrCrC-3′; and FK224, 5′-rGrGrCrCrArUrGrGrArArCrArGrGrUrArGrUrUrUrUrCrCrArG-3′. These oligonucleotides were derived from green fluorescent protein. Various forms of 25-nucleotide dsRNA were generated by annealing different combinations of these oligonucleotides: 25-nucleotide dsRNA with 5′ 2-nucleotide overhang, FK221 with FK222; blunt end, FK221 with FK223; and 3′ 2-nucleotide overhang, FK221 with FK224. Protocols for annealing and validation of dsRNA formation were as described (Elbashir et al., 2002). Labeling of the 5′ ends of the 25-nucleotide ssRNAs and dsRNAs with ^{32}P was performed with T4 polynucleotide kinase (New England Biolabs).

RNase Assay

Single-stranded specific RNase assays were performed as follows. Briefly, 5′-^{32}P-radiolabeled ssRNA, dsRNA, or phloem sap–purified small RNA was incubated with 1 ng of RNase A and 1 unit of RNase T1 (Ambion) in 10 μL of RNase digestion buffer (300 mM NaCl, 50 mM Tris, pH 7.0, and 1 mM EDTA) at 37°C for 30 min. The reaction mixtures were then analyzed by denaturing PAGE (7 M urea/15% PAGE gel) and autoradiography.

Cloning, Sequencing, and Bioinformatics of Small RNA

Phloem sap small RNA was isolated and purified as described. This population of small RNA was ligated to adapters and amplified by RT-PCR according to established procedures (Elbashir et al., 2001). Adapter and primer sequences were as described (Elbashir et al., 2001), with the exception that adaptors were fluorescently tagged (3′ fluorescein for the 3′ adaptor and 5′ Cy5 for the 5′ adaptor). Ligation products were visualized using a Typhoon scanner (Model 9400; Amersham Biosciences) or by a UV transilluminator. The amplified sequences were gel purified and cloned into pCR4-TOPO vector (Invitrogen), followed by electroporation into *Escherichia coli* DH10B cells.

The transformants (~10,000 clones) were sequenced with the BigDye terminator cycle sequencing kit (PE Applied Biosystems, Foster City, CA). These sequences were first analyzed to establish the size class distribution of the phloem subpopulation of small RNA. Redundancy was established using BLASTN (http://www.ncbi.nlm.nih.gov/BLAST/) to compare each clone in this database against every other small RNA sequence. Potential rRNA and tRNA contaminants were screened based on the detection of small RNAs having close identity (0 to 3 nucleotide changes) to *Arabidopsis thaliana* rRNA and tRNA sequences (http://www.expasy.org/cgi-bin/lists?ribosomp.txt; http://rna.wustl.edu/GtRDB/At/At-seqs.html) or cucurbit rRNA sequences. Only a small fraction of the 10,000 clones (~2%) was identified as being derived from tRNA and rRNA. This finding indicates that the small RNA population was not contaminated with companion cell-derived tRNA/rRNA degradation products. Putative miRNA candidates were identified on the basis of phylogenetic conservation as sequences with 0 to 3 nucleotide changes to Arabidopsis intergenic region sequences (TAIR Arabidopsis intergenic sequences; http://arabidopsis.org).

Identity of potential target sequences was probed by conducting FASTA analyses with each sequence and its reverse complement against proprietary ESTs (Genesis Research and Development plant consensi, including sequences from Actinidia, Cucurbita, Eucalyptus, Festuca, Lolium, *Malus domestica*, *Pinus radiata*, and Vaccinium [349,411 sequences]) and public plant EST databases, including *Chlamydomonas reinhardtii*, *Glycine max*, Gossypium, *Lycopersicon esculentum*, *Medicago truncatula*, *Pinus taeda*, *Triticum aestivum*, *Vitis vinifera*, *Zea mays* (The Institute for Genomic Research gene indices [http://www.tigr.org]; 412,390 sequences), and Arabidopsis coding sequences (TAIR Arabidopsis coding sequences; http://arabidopsis.org). Sequences within each of these data sets were then mapped by TBLASTX against Arabidopsis genes (TAIR CDS; http://arabidopsis.org). Criteria used to identify putative miRNA targets included (1) a reverse orientation match to an Arabidopsis gene, (2) instances where mapping onto the same (or similar) Arabidopsis genes was observed from two or more species, and (3) manual inspection of the Arabidopsis gene annotation in instances where multiple Arabidopsis gene identifiers were involved. For access to the AgriGenesis phloem small RNA database, contact Tony Lough (t.lough@agrigenesis.co.nz).

Identified conserved sequences were further analyzed by an RNA-folding program (RNAFold from Vienna package, version 1.4; http://www.tbi.univie.ac.at/~ivo/RNA/]). This allowed for the identification of candidates with a potential fold-back precursor structure that contain an miRNA sequence within one arm of the hairpin. These small RNA candidates were confirmed both by in silico and transcriptional profiling of phloem miRNA using RNA gel blotting analysis. Parallel analyses were performed on small RNA cloned from the phloem sap collected from viral-infected greenhouse-grown (summer) pumpkin plants. The virus used in these experiments was CuYV, and its presence in the phloem sap was confirmed by RT-PCR using standard molecular protocols. Phloem sap used in these studies was collected from plants showing clear symptoms of virus infection. Sequence identity of each clone was established using BLASTN against the CuYV sequence (GenBank accession numbers AB085612 [RNA 1] and AB085613 [RNA 2]). Size class analysis was performed as described.

RNA Gel Blot and RT-PCR Analyses

Analysis of leaf full-length *CP* transcripts was performed as follows: total RNA was extracted from mature squash leaves with TRIzol reagent, separated on a formaldehyde-containing 1% agarose gel (10 μg of total RNA/lane), and transferred overnight to a Hybond-N$^+$ nylon membrane (Amersham Biosciences). The membrane was UV cross-linked and prehybridized at 65°C for 1 h in hybridization buffer (0.5 M Na_2HPO_4, 1 mM EDTA, 1% BSA, and 7% SDS), before being hybridized overnight with full-length SqMV *CP* DNA probe that was radiolabeled by random priming (NEN, Boston, MA). The membrane was then washed (2 × 15 min at 65°C) in 2× SSC (1× SSC is 0.15 M NaCl and 0.015 M sodium citrate) and again (2 × 15 min) in 0.1× SSC, followed by exposure to x-ray film for 12 h at −80°C. Equal loading was confirmed by stripping the membrane in 0.1% SDS at 95°C and reprobing with a squash 18S rRNA DNA probe.

RNA gel blot analysis of the enriched small RNA preparation was performed as follows. RNA was separated on a denaturing polyacrylamide gel, urea removed and the RNA stained with ethidium bromide to visualize the amounts loaded. RNA was then transferred to Hybond-N$^+$ nylon membrane using a *trans*-blot SD cell (Bio-Rad, Hercules, CA; 1 h at 3 mA/cm^2). Prehybridization and hybridization were as described, except that the temperature was 45°C, and the probe was either full-length sense or antisense *SqMV CP* RNA, generated by in vitro transcription using SP6 or T7 RNA polymerase (Ambion), respectively. The membrane was washed (2 × 10 min, 50°C in 2× SSC, 0.1% SDS) and then exposed to x-ray film overnight at −80°C.

RNA gel blot analyses of cucurbit miRNA were performed as described, with the exception that DNA sense or antisense probes were end labeled by the forward reaction using 10 units of T4 polynucleotide kinase (New England Biolabs) with the supplied buffer, to which was added 300 nM [γ-^{32}P]ATP (3000 Ci/mmol) for 10 min at 37°C. Unincorporated ^{32}P-label was removed using a ProbeQuant G-50 microcolumn (Amersham Biosciences), according to the manufacturer's instructions. Hybridization signal was detected using a Typhoon scanner.

RT-PCR analysis of phloem sap RNA was performed as follows. An aliquot (3 μL) of the high molecular weight RNA (obtained by Qiagen column size-fractionation) was used in RT-PCR with SuperScriptII RT (Invitrogen) according to the manufacturer's recommendations, with the following gene-specific primers: *CmPP16-3′*, 5′-ATGGGTTTGAAGAAGCCAAGCCACTTA-3′; *rbcS-3′*, 5′-TTGTCGAAGCCAATGACTCTGATGAA-3′; SqMV*CP-3′*, 5′-CATGGAGCTAGATCTTGCGCAACTTTCTCTG-3′. An aliquot (3 μL) of the RT reaction was used for PCR amplification, with the following conditions: 5 min at 95°C (1 cycle); 30 s at 94°C, 30 s at 60°C, and 90 s at 72°C (35 cycles). The same 3′ primers were used as for the RT reaction, in addition to the following 5′ primers: *CmPP16-5′*, 5′-GTGGTAAAGGACTTCAAGCCCACGACC-3′; *rbcS-5′*, 5′-ATGGCTTCCATCGTCTCATCCGCC-3′; SqMV*CP-5′*, 5′-CATGGTACAGCAGCTTGGAACTTATATTCCA-3′. Full-length SqMV *CP* was amplified using the above-described primer set. The presence of smaller SqMV*CP* fragments was probed using a series of internal primer sets that were evenly spaced along the entire *CP* coding region.

Anion-Exchange Chromatography and RNA Overlay Analysis of Phloem Sap Proteins

Anion-exchange chromatography of pumpkin, cucumber, and lupin phloem sap proteins was performed as follows. Generally, 20 mL of pumpkin or cucumber phloem sap (10 to 20 mg/mL) or 45 mL of lupin phloem sap (0.1 to 0.2 mg/mL) was employed for the chromatographic separation of phloem proteins. Phloem sap was first dialyzed against buffer A (50 mM Tris, pH 7.5, 1 mM EDTA, and 30 mM 2-mercaptoethanol) and clarified by centrifugation (17,000*g* for 30 min). Phloem proteins were then loaded onto a buffer A–equilibrated HiTrap Q column, connected to an FPLC system (Amersham Biosciences). After washing the column with 20 column volumes of buffer A, proteins were eluted with a linear gradient of 0 to 500 mM NaCl in buffer A supplemented with 1 M NaCl.

For northwestern analysis, phloem proteins in each of the HiTrap-Q fractions were resolved by 13% SDS-PAGE and then electrotransferred to nitrocellulose membrane. After staining with Ponceau S, to mark the lanes and molecular weight markers, membranes were thoroughly washed first with TBS (50 mM Tris, pH 8.0, and 500 mM NaCl), followed by DEPC-treated Milli-Q water (Millipore, Bedford, MA). Washed membranes were further rinsed, briefly, with 10 mL of RNA binding buffer ([RBB]; 10 mM Tris, pH 7.0, 50 mM KCl, 1 mM EDTA, 0.02% [w/v] Ficoll, and 0.02% [w/v] polyvinylpyrrolidone) and blocked at 25°C for 1 h with 10 mL of the RBB supplemented with 0.02% (v/v) ultrapure BSA (Ambion) and 0.1 mg/mL of yeast total RNA. Next, membranes were rinsed (2 × 10 min) with RBB supplemented only with BSA. Hybridization was performed with ^{32}P-labeled probes (2 × 10^5 cpm/mL) in 7 mL of RBB supplemented with BSA at 25°C for 1 h. Membranes were then washed (3 × 5 min) with RBB, briefly air dried, and autoradiographed.

PSRP1 Purification and Mass Spectroscopic Analysis

All protein purification steps were performed at 4°C. Phloem proteins were fractionated by anion-exchange chromatography, as described, and then analyzed by a combination of SDS-PAGE/GelCode Blue staining (Pierce, Rockford, IL) and northwestern assays to locate PSRP1-containing fractions. Next, metal chelation chromatography was employed, based on our results for amino acid composition analysis (Molecular Structure Facility, University of California, Davis) that revealed a high content of His in this protein. For this purpose, fractions were pooled, the NaCl concentration adjusted to 500 mM, and this preparation loaded onto a metal chelation column (Novagen, Madison, WI) equilibrated with binding buffer (20 mM Tris, pH 8.0, 500 mM NaCl, and 10 mM imidazole). After washing with 20 column volumes of the washing buffer containing 60 mM imidazole, PSRP1 was eluted with a buffer solution containing 400 mM imidazole. Remaining PSRP1 was then released using a second elution buffer (20 mM Tris, pH 8.0, 150 mM NaCl, and 100 mM EDTA). Mass spectroscopic analysis of phloem-purified PSRP1 was performed using matrix-assisted laser desorption ionization time-of-flight on a Biflex III system (Bruker, Billerica, MA) as described (Yoo et al., 2002).

PSRP1 Cloning from Pumpkin

PSRP1 was recalcitrant to commonly used endoproteinases. To resolve this problem, phloem-purified PSRP1 (1 μg) was digested for 2 h at 25°C with a less specific proteinase, chymotrypsin (0.1 μg), in 20 μL of digestion buffer (100 mM Hepes, pH 8.0, and 10 mM $CaCl_2$). Resultant peptides were then resolved on a 15% nondenaturing tricine PAGE gel, electroblotted to a polyvinylidene difluoride membrane, stained with Coomassie Brilliant Blue R 250, and then subjected to Edman sequencing (Molecular Structure Facility). The following two microsequences were obtained: HGP(G/S)(P/H)G(P/H)A(G/H)G(H/P)(G/S)GPA and GHGP(A/S)GGHGH(G/H)P(A/S)A. Pumpkin stem mRNA was used in RT-PCR with the degenerate primers 5′-GGICAYGGICCIGCIGGIGGICAYGGICA-3′ and 5′-CAYGGICCIGGICCIGGICCIGCIGGIGGICAY-3′ (I, inosine; Y, U/C). Cloning required a high temperature of 60°C for reverse transcription, using Thermoscript RT (Invitrogen), to yield a specific PCR product of 450 bp. This experimental condition was consistent with the high G/C content of *PSRP1*. The resultant PCR product was then used as a probe to screen a pumpkin stem cDNA library (Yoo et al., 2002). After three cycles of screening, nine positive plaques were purified from ~1.5 × 10^5 pfu; cDNA inserts were then rescued in pBK-CMV by in vivo excision followed by sequencing.

Expression and Purification of Recombinant PSRP1

For expression and purification of recombinant (R)-PSRP1, an expression vector, pET15b-PSRP1, was constructed: an *Nco*I-*Xho*I fragment from pBK-CMV/PSRP1 was ligated into pET15b, which was previously digested with *Nco*I and *Xho*I, and dephosphorylated with calf intestinal alkaline phosphatase. The resultant plasmid, pET15b-PSRP1, permitted expression of PSRP1, as a native protein, without a $(His)_6$ fusion. *E. coli*, BL21(DE3)pLysS, harboring pET15b-PSRP1, was induced with 0.5 mM isopropylthio-β-galactoside for 2 to 3 h at 22°C. For purification, cells were lysed by sonication (four to six pulses for 1 min each using a Sonic Dismembrator; Fisher Scientific, Pittsburgh, PA) and centrifuged at 20,000*g* for 30 min at 4°C. The cleared supernatant was then applied to a metal chelation column, and R-PSRP1 was purified as described.

In Situ RT-PCR Detection of PSRP1

Tissue localization of *CmPSRP1* was determined using established protocols for in situ RT-PCR (Ruiz-Medrano et al., 1999). The primer pair used to amplify *PSRP1* transcripts was as follows: forward primer, 5′-CTAATCTTTGCATCCATGGCGTCTTTCCAATGC-3′; reverse primer, 5′-TTAGTGCTGACCTCTGCGACAATCGTTGTCAC-3′. The pattern associated with *CmPP16* was determined using the following primer pair: forward primer, 5′-GTGGTAAAGGACTTCAAGCCCACGACC-3′; reverse primer, 5′-ATGGGTTTGAAGAAGCCAAGCCACTTA-3′. Controls for these studies were performed in the absence of the appropriate primers.

Protein Gel Blot Analysis

Primary antibody used to detect PSRP1, and its probable homologs in other plant species, was a monoclonal anti-His_6 antibody (Covance, Berkeley, CA). This antibody efficiently recognized PSRP1 and its homologs in protein gel blot analyses because of their high His content. Routine protocols for protein gel blot analysis were followed. Briefly, nitrocellulose membranes were blocked, with 5% nonfat milk made in TBS, for 0.5 to 1 h, incubated with the primary antibody for 1 h, washed four times with TTBS (TBS supplemented with 0.5% [v/v] Tween 20) for 5 min each, and then incubated for 30 min with secondary antibodies conjugated to horseradish peroxidase (KPL, Gaithersburg, MD). Membranes were then washed as described. Visualization of antigen and antibody complexes was achieved using luminol and oxidizing reagents (Renaissance; PerkinElmer Life Sciences, Boston, MA) as substrates for the horseradish peroxidase.

Electrophoretic Mobility-Shift Assays

Electrophoretic mobility-shift assays were performed as described (Smith, 1998). Reactions were assembled on ice in 10 μL of binding buffer (20 mM Hepes, pH 8.0, 50 mM KCl, 1 mM DTT, and 5% [v/v] glycerol). An equal amount (10 fmol) of ^{32}P end-labeled 25-nucleotide ssRNA or dsRNA was used in assays with various concentrations of

purified and desalted R-PSRP1. Reaction mixtures were incubated on ice for 25 min and then resolved on a 5% (v/v) nondenaturing polyacrylamide gel that was prerun for 30 min at 100 V. Electrophoresis was performed at 4°C and 200 V. The gel was then dried and phospho-imaged using a Typhoon 8600 variable mode imager (Amersham Biosciences). Competition assays were performed essentially as described for the electrophoretic mobility-shift assays, except that R-PSRP1 was first incubated with various amounts of unlabeled ssRNA for 10 min, followed by the addition of radioactively labeled 25-nucleotide ssRNA and further incubation for 15 min. Quantitation of the phospho-images was performed using ImageQuant Tools software, version 3.3 (Amersham Biosciences).

Microinjection Experiments

RNA molecules for use in microinjection experiments were labeled either with Alexa Fluor 488 or 568 using the ULYSIS nucleic acid labeling kit (Molecular Probes) according to the manufacturer's protocol. Unincorporated fluorescent label was separated by repeated ethanol precipitation or by a G-25 gel filtration column (Amersham Biosciences). The integrity of fluorescently labeled probes was verified by 3% (w/v) agarose gel electrophoresis and fluorescence imaging. Recombinant KN1 (R-KN1) and CMV-MP (R-CMV-MP) were expressed in and isolated from *E. coli* as previously described (Lucas et al., 1995; Rojas et al., 1997).

Eight-week-old *Nicotiana benthamiana* plants were used for microinjection studies, with a minimum of five plants for each probe tested. Leaves (3 to 5 cm in length) were excised and prepared for microinjection experiments as described (Rojas et al., 1997). Fluorescently labeled RNA was resuspended with 1 to 3 μg/μL of purified protein solution to yield a final RNA concentration of 1 to 2 μg/μL. Fluorescein isothiocyanate–labeled dextran (20-kD FITC-dextran; Sigma, St. Louis, MO) was mixed with protein to give a final concentration of 2 mM. All probes were stored at 4°C, and integrity of RNA was confirmed before use in each microinjection experiment. Microinjection protocols were as previously described (Rojas et al., 1997), and probes were introduced via pressure-mediated delivery. Cell-to-cell movement of fluorescently labeled probes was observed using a confocal laser-scanning microscope (model DM RXE TCS-4D; Leica, Heidelberg, Germany). Spatial distribution of fluorescence within the mesophyll tissue was evaluated for a 20-min period after the probe(s) was introduced into a target cell. Images were simultaneously collected for the fluorescent signals emitted in the FITC/Alexa Fluor 488 nm (green), Alexa Flour 568 nm (red), and chlorophyll 665 nm (blue) channels. Optical sections were stacked and then combined to generate the images presented.

Sequence data from this article have been deposited with the EMBL/GenBank data libraries under accession numbers AB085612 (RNA 1), AB085613 (RNA 2), At2g32460, AF237633, O80326, AF156667, and AY326308.

ACKNOWLEDGMENTS

We thank Roberto Ruiz-Medrano for his contributions to preliminary phloem small RNA studies, Nien-Chen Huang, David Tricoli, Alex Adai, and Ilkk Havukala for expert assistance, and the members of the Lucas lab for helpful discussions. This work was supported by grants (to W.J.L.) from the National Science Foundation (IBN 03151174) and the Department of Energy, Division of Energy Biosciences (DE-FG03-94ER20134).

Received April 22, 2004; accepted May 6, 2004.

REFERENCES

Aoki, K., Kragler, F., Xoconostle-Cázares, B., and Lucas, W.J. (2002). A subclass of plant heat shock cognate 70 chaperones carries a motif that facilitates trafficking through plasmodesmata. Proc. Natl. Acad. Sci. USA **99,** 16342–16347.

Atkins, C.A. (1999). Spontaneous phloem exudation accompanying abscission in *Lupinus mutabilis* (Sweet). J. Exp. Bot. **50,** 805–812.

Aukerman, M.J., and Sakai, H. (2003). Regulation of flowering time and floral organ identity by a microRNA and its APETALA2-like target genes. Plant Cell **15,** 2730–2741.

Balachandran, S., Xiang, Y., Schobert, C., Thompson, G.A., and Lucas, W.J. (1997). Phloem sap proteins from *Cucurbita maxima* and *Ricinus communis* have the capacity to traffic cell to cell through plasmodesmata. Proc. Natl. Acad. Sci. USA **94,** 14150–14155.

Bartel, B., and Bartel, D.P. (2003). MicroRNAs: At the root of plant development? Plant Physiol. **132,** 709–717.

Bernstein, E., Caudy, A.A., Hammond, S.M., and Hannon, G.J. (2001). Role for a bidentate ribonuclease in the initiation step of RNA interference. Nature **409,** 363–366.

Carrington, J.C., and Ambros, V. (2003). Role of microRNAs in plant and animal development. Science **301,** 336–338.

Carrington, J.C., Kasschau, K.D., Mahajan, S.K., and Schaad, M.C. (1996). Cell-to-cell and long-distance transport of viruses in plants. Plant Cell **8,** 1669–1681.

Dalmay, T., Hamilton, A., Rudd, S., Angell, S., and Baulcombe, D.C. (2000). An RNA-dependent RNA polymerase gene in *Arabidopsis* is required for posttranscriptional gene silencing mediated by a transgene but not by a virus. Cell **101,** 543–553.

Dalmay, T., Horsefield, R., Braunstein, T.H., and Baulcombe, D.C. (2001). SDE3 encodes an RNA helicase required for posttranscriptional gene silencing in *Arabidopsis*. EMBO J. **20,** 2069–2077.

Di Serio, F., Schob, H., Iglesias, A., Tarina, C., Bouldoires, E., and Meins, F. (2001). Sense- and antisense-mediated gene silencing in tobacco is inhibited by the same viral suppressors and is associated with accumulation of small RNAs. Proc. Natl. Acad. Sci. USA **98,** 6506–6510.

Elbashir, S.M., Harborth, J., Weber, K., and Tuschl, T. (2002). Analysis of gene function in somatic mammalian cells using small interfering RNAs. Methods **26,** 199–213.

Elbashir, S.M., Lendeckel, W., and Tuschl, T. (2001). RNA interference is mediated by 21-and 22-nucleotide RNAs. Genes Dev. **15,** 188–200.

Fagard, M., and Vaucheret, H. (2000). (Trans)gene silencing in plants: How many mechanisms? Annu. Rev. Plant Physiol. Plant Mol. Biol. **51,** 167–194.

Fire, A., Xu, S.Q., Montgomery, M.K., Kostas, S.A., Driver, S.E., and Mello, C.C. (1998). Potent and specific genetic interference by double-stranded RNA in *Caenorhabditis elegans*. Nature **391,** 806–811.

Fisher, D.B., Wu, Y., and Ku, M.S.B. (1992). Turnover of soluble proteins in the wheat sieve tube. Plant Physiol. **100,** 1433–1441.

Foster, T.M., Lough, T.J., Emerson, S.J., Lee, R.H., Bowman, J.L., Forster, R.L.S., and Lucas, W.J. (2002). A surveillance system regulates selective entry of RNA into the shoot apex. Plant Cell **14,** 1497–1508.

Gilbertson, R.L., and Lucas, W.J. (1996). How do viruses traffic on the 'vascular highway'? Trends Plant Sci. **1,** 260–268.

Golecki, B., Schulz, A., Carstens-Behrens, U., and Kollmann, R. (1998). Evidence for graft transmission of structural phloem proteins or their precursors in heterografts of *Cucurbitaceae*. Planta **206,** 630–640.

Golecki, B., Schulz, A., and Thompson, G.A. (1999). Translocation of structural P proteins in the phloem. Plant Cell **11,** 127–140.

Guo, H.S., and Ding, S.W. (2002). A viral protein inhibits the long range signaling activity of the gene silencing signal. EMBO J. **21,** 398–407.

Hamilton, A., Voinnet, O., Chappell, L., and Baulcombe, D. (2002). Two classes of short interfering RNA in RNA silencing. EMBO J. **21,** 4671–4679.

Hamilton, A.J., and Baulcombe, D.C. (1999). A species of small antisense RNA in posttranscriptional gene silencing in plants. Science **286,** 950–952.

Hammond, S.M., Bernstein, E., Beach, D., and Hannon, G.J. (2000). An RNA-directed nuclease mediates post-transcriptional gene silencing in *Drosophila* cells. Nature **404,** 293–296.

Hannon, G.J. (2002). RNA interference. Nature **418,** 244–251.

Hartono, S., Natsuaki, T., Genda, Y., and Okuda, S. (2003). Nucleotide sequence and genome organization of *Cucumber yellows virus*, a member of the genus Crinivirus. J. Gen. Virol. **84,** 1007–1012.

Haywood, V., Kragler, F., and Lucas, W.J. (2002). Plasmodesmata: Pathways for protein and ribonucleoprotein signaling. Plant Cell **14** (suppl.), S303–S325.

Himber, C., Dunoyer, P., Moissiard, G., Ritzenthaler, C., and Voinnet, O. (2003). Transitivity-dependent and -independent cell-to-cell movement of RNA silencing. EMBO J. **22,** 4523–4533.

Hutvagner, G., McLachlan, J., Pasquinelli, A.E., Balint, E., Tuschl, T., and Zamore, P.D. (2001). A cellular function for the RNA-interference enzyme Dicer in the maturation of the let-7 small temporal RNA. Science **293,** 834–838.

Hutvagner, G., and Zamore, P.D. (2002). A microRNA in a multiple-turnover RNAi enzyme complex. Science **297,** 2056–2060.

Jackson, D. (2000). Opening up the communication channels: Recent insights into plasmodesmal function. Curr. Opin. Plant Biol. **3,** 394–399.

Jeschke, W.D., and Pate, J.S. (1991). Cation and chloride partitioning through xylem and phloem within the whole plant of *Ricinus communis* L. under conditions of salt stress. J. Exp. Bot. **42,** 1105–1116.

Jorgensen, R.A., Atkinson, R.G., Forster, R.L.S., and Lucas, W.J. (1998). An RNA-based information superhighway in plants. Science **279,** 1486–1487.

Kasschau, K.D., Xie, Z.X., Allen, E., Llave, C., Chapman, E.J., Krizan, K.A., and Carrington, J.C. (2003). P1/HC-Pro, a viral suppressor of RNA silencing, interferes with *Arabidopsis* development and miRNA function. Dev. Cell **4,** 205–217.

Khvorova, A., Reynolds, A., and Jayasena, S.D. (2003). Functional siRNAs and miRNAs exhibit strand bias. Cell **115,** 209–216.

Kidner, C.A., and Martienssen, R.A. (2003). Macro effects of microRNAs in plants. Trends Genet. **19,** 13–16.

Kim, J.Y., Yuan, Z.A., Cilia, M., Khalfan-Jagani, Z., and Jackson, D. (2002). Intercellular trafficking of a KNOTTED1 green fluorescent protein fusion in the leaf and shoot meristem of Arabidopsis. Proc. Natl. Acad. Sci. USA **99,** 4103–4108.

Kim, J.Y., Yuan, Z., and Jackson, D. (2003). Developmental regulation and significance of KNOX protein trafficking in *Arabidopsis*. Development **130,** 4351–4362.

Kim, M., Canio, W., Kessler, S., and Sinha, N. (2001). Developmental changes due to long-distance movement of a homeobox fusion transcript in tomato. Science **293,** 287–289.

Klahre, U., Crete, P., Leuenberger, S.A., Iglesias, V.A., and Meins, F. (2002). High molecular weight RNAs and small interfering RNAs induce systemic posttranscriptional gene silencing in plants. Proc. Natl. Acad. Sci. USA **99,** 11981–11986.

Knoblauch, M., and van Bel, A.J.E. (1998). Sieve tubes in action. Plant Cell **10,** 35–50.

Lewis, B.P., Shih, I.H., Jones-Rhoades, M.W., Bartel, D.P., and Burge, C.B. (2003). Prediction of mammalian microRNA targets. Cell **115,** 787–798.

Lim, L.P., Lau, N.C., Weinstein, E.G., Abdelhakim, A., Yekta, S., Rhoades, M.W., Burge, C.B., and Bartel, D.P. (2003). The microRNAs of *Caenorhabditis elegans*. Genes Dev. **17,** 991–1008.

Llave, C., Kasschau, K.D., Rector, M.A., and Carrington, J.C. (2002b). Endogenous and silencing-associated small RNAs in plants. Plant Cell **14,** 1605–1619.

Llave, C., Xie, Z.X., Kasschau, K.D., and Carrington, J.C. (2002a). Cleavage of Scarecrow-like mRNA targets directed by a class of Arabidopsis miRNA. Science **297,** 2053–2056.

Lucas, W.J. (1995). Plasmodesmata: Intercellular channels for macromolecular transport in plants. Curr. Opin. Cell Biol. **7,** 673–680.

Lucas, W.J., Bouché-Pillon, S., Jackson, D.P., Nguyen, L., Baker, L., Ding, B., and Hake, S. (1995). Selective trafficking of KNOTTED1 homeodomain protein and its mRNA through plasmodesmata. Science **270,** 1980–1983.

Lucas, W.J., Yoo, B.-C., and Kragler, F. (2001). RNA as a long-distance information macromolecule in plants. Nat. Rev. Mol. Cell Biol. **2,** 849–857.

Mallory, A.C., Ely, L., Smith, T.H., Marathe, R., Anandalakshmi, R., Fagard, M., Vaucheret, H., Pruss, G., Bowman, L., and Vance, V.B. (2001). HC-Pro suppression of transgene silencing eliminates the small RNAs but not transgene methylation or the mobile signal. Plant Cell **13,** 571–583.

Mallory, A.C., Mlotshwa, S., Bowman, L.H., and Vance, V.B. (2003). The capacity of transgenic tobacco to send a systemic RNA silencing signal depends on the nature of the inducing transgene locus. Plant J. **35,** 82–92.

Mlotshwa, S., Voinnet, O., Mette, M.F., Matzke, M., Vaucheret, H., Ding, S.W., Pruss, G., and Vance, V.B. (2002). RNA silencing and the mobile silencing signal. Plant Cell **14** (suppl.), S289–S301.

Mourrain, P., et al. (2000). *Arabidopsis SGS2* and *SGS3* genes are required for posttranscriptional gene silencing and natural virus resistance. Cell **101,** 533–542.

Nakajima, K., Sena, G., Nawy, T., and Benfey, P.N. (2001). Intercellular movement of the putative transcription factor SHR in root patterning. Nature **413,** 307–311.

Olsen, P.H., and Ambros, V. (1999). The *lin-4* regulatory RNA controls developmental timing in *Caenorhabditis elegans* by blocking LIN-14 protein synthesis after the initiation of translation. Dev. Biol. **216,** 671–680.

Palatnik, J.F., Allen, E., Wu, X.L., Schommer, C., Schwab, R., Carrington, J.C., and Weigel, D. (2003). Control of leaf morphogenesis by microRNAs. Nature **425,** 257–263.

Palauqui, J.-C., Elmayan, T., Pollien, J.-M., and Vaucheret, H. (1997). Systemic acquired silencing: Transgene-specific post-transcriptional silencing is transmitted by grafting from silenced stocks to non-silenced scions. EMBO J. **16,** 4738–4745.

Pang, S.Z., Jan, F.J., Tricoli, D.M., Russell, P.F., Carney, K.J., Hu, J.S., Fuchs, M., Quemada, H.D., and Gonsalves, D. (2000). Resistance to squash mosaic comovirus in transgenic squash plants expressing its coat protein genes. Mol. Breeding **6,** 87–93.

Papp, I., Mette, M.F., Aufsatz, W., Daxinger, L., Schauer, S.E., Ray, A., van der Winden, J., Matzke, M., and Matzke, A.J.M. (2003). Evidence for nuclear processing of plant micro RNA and short interfering RNA precursors. Plant Physiol. **132,** 1382–1390.

Reinhart, B.J., Weinstein, E.G., Rhoades, M.W., Bartel, B., and Bartel, D.P. (2002). MicroRNAs in plants. Genes Dev. **16,** 1616–1626.

Rhoades, M.W., Reinhart, B.J., Lim, L.P., Burge, C.B., Bartel, B., and Bartel, D.P. (2002). Prediction of plant microRNA targets. Cell **110,** 513–520.

Robards, A.W., and Lucas, W.J. (1990). Plasmodesmata. Annu. Rev. Plant Physiol. Plant Mol. Biol. **41,** 369–419.

Roignant, J.Y., Carre, C., Mugat, R., Szymczak, D., Lepesant, J.A., and Antoniewski, C. (2003). Absence of transitive and systemic pathways allows cell-specific and isoform-specific RNAi in *Drosophila*. RNA **9,** 299–308.

Rojas, M.R., Zerbini, F.M., Allison, R.F., Gilbertson, R.L., and Lucas, W.J. (1997). Capsid protein and helper component proteinase function as potyvirus cell-to-cell movement proteins. Virology **237,** 283–295.

Rudenko, G.N., Ono, A., and Walbot, V. (2003). Initiation of silencing of maize MuDR/Mu transposable elements. Plant J. **33,** 1013–1025.

Ruiz-Medrano, R., Xoconostle-Cázares, B., and Lucas, W.J. (1999). Phloem long-distance transport of *CmNACP* mRNA: Implications for supracellular regulation in plants. Development **126,** 4405–4419.

Sambrook, J., Fritsch, E.F., and Maniatis, T. (1989). Molecular Cloning: A Laboratory Manual. (Cold Spring Harbor, NY: Cold Spring Harbor Laboratory Press).

Schauer, S.E., Jacobsen, S.E., Meinke, D.W., and Ray, A. (2002). DICER-LIKE1: Blind men and elephants in *Arabidopsis* development. Trends Plant Sci. **7,** 487–491.

Schiefelbein, J. (2003). Cell-fate specification in the epidermis: A common patterning mechanism in the root and shoot. Curr. Opin. Plant Biol. **6,** 74–78.

Sessions, A., Yanofsky, M.F., and Weigel, D. (2000). Cell-cell signaling and movement by the floral transcription factors LEAFY and APETALA1. Science **289,** 779–781.

Sijen, T., Fleenor, J., Simmer, F., Thijssen, K.L., Parrish, S., Timmons, L., Plasterk, R.H.A., and Fire, A. (2001). On the role of RNA amplification in dsRNA-triggered gene silencing. Cell **107,** 465–476.

Silhavy, D., Molnar, A., Lucioli, A., Szittya, G., Hornyik, C., Tavazza, M., and Burgyan, J. (2002). A viral protein suppresses RNA silencing and binds silencing-generated, 21- to 25-nucleotide double-stranded RNAs. EMBO J. **21,** 3070–3080.

Smith, C.W.J. (1998). RNA: Protein Interactions. (New York: Oxford University Press).

Tang, G.L., Reinhart, B.J., Bartel, D.P., and Zamore, P.D. (2003). A biochemical framework for RNA silencing in plants. Genes Dev. **17,** 49–63.

van Bel, A.J.E. (2003). The phloem—A miracle of ingenuity. Plant Cell Environ. **26,** 125–149.

Vance, V., and Vaucheret, H. (2001). RNA silencing in plants—Defense and counterdefense. Science **292,** 2277–2280.

Vargason, J.M., Szittya, G., Burgyan, J., and Hall, T.M.T. (2003). Size selective recognition of siRNA by an RNA silencing suppressor. Cell **115,** 799–811.

Voinnet, O. (2001). RNA silencing as a plant immune system against viruses. Trends Genet. **17,** 449–459.

Voinnet, O., Pinto, Y.M., and Baulcombe, D.C. (1999). Suppression of gene silencing: A general strategy used by diverse DNA and RNA viruses of plants. Proc. Natl. Acad. Sci. USA **96,** 14147–14152.

Voinnet, O., Vain, P., Angell, S., and Baulcombe, D.C. (1998). Systemic spread of sequence-specific transgene RNA degradation in plants is initiated by localized introduction of ectopic promoterless DNA. Cell **95,** 177–187.

Volpe, T.A., Kidner, C., Hall, I.M., Teng, G., Grewal, S.I.S., and Martienssen, R.A. (2002). Regulation of heterochromatic silencing and histone H3 lysine-9 methylation by RNAi. Science **297,** 1833–1837.

Wada, T., Kurata, T., Tominaga, R., Koshino-Kimura, Y., Tachibana, T., Goto, K., Marks, M.D., Shimura, Y., and Okada, K. (2002). Role of a positive regulator of root hair development, CAPRICE, in *Arabidopsis* root epidermal cell differentiation. Development **129,** 5409–5419.

Wassenegger, M. (2002). Gene silencing. Int. Rev. Cytol. **219,** 61–113.

Winston, W.M., Molodowitch, C., and Hunter, C.P. (2002). Systemic RNAi in *C. elegans* requires the putative transmembrane protein SID-1. Science **295,** 2456–2459.

Wu, X.L., Weigel, D., and Wigge, P.A. (2002). Signaling in plants by intercellular RNA and protein movement. Genes Dev. **16,** 151–158.

Xoconostle-Cázares, B., Xiang, Y., Ruiz-Medrano, R., Wang, H.-L., Monzer, J., Yoo, B.C., McFarland, K.C., Franceschi, V.R., and Lucas, W.J. (1999). Plant paralog to viral movement protein that potentiates transport of mRNA into the phloem. Science **283,** 94–98.

Ye, K.Q., Malinina, L., and Patel, D.J. (2003). Recognition of small interfering RNA by a viral suppressor of RNA silencing. Nature **426,** 874–878.

Yoo, B.C., Lee, J.Y., and Lucas, W.J. (2002). Analysis of the complexity of protein kinases within the phloem sieve tube system. Characterization of *Cucurbita maxima* CALMODULIN-LIKE DOMAIN PROTEIN KINASE 1. J. Biol. Chem. **277,** 15325–15332.

Zambryski, P., and Crawford, K. (2000). Plasmodesmata: Gatekeepers for cell-to-cell transport of developmental signals in plants. Annu. Rev. Cell Dev. Biol. **16,** 393–421.

Zamore, P.D. (2002). A surveillance system regulates selective entry of RNA into the shoot apex: Ancient pathways programmed by small RNAs. Science **296,** 1265–1269.

Zamore, P.D., Tuschl, T., Sharp, P.A., and Bartel, D.P. (2000). RNAi: Double-stranded RNA directs the ATP-dependent cleavage of mRNA at 21 to 23 nucleotide intervals. Cell **101,** 25–33.